Evaluation of Room Temperature Vulcanized (RTV) Silicone Rubber Coated Porcelain Post Insulators under Contaminated Conditions

by

Vipul Gholap

A Thesis Presented in Partial Fulfillment
of the Requirements for the Degree
Master of Science

Approved January 2013 by the
Graduate Supervisory Committee:

Ravi Gorur, Chair
George Karady
Raja Ayyanar

ARIZONA STATE UNIVERSITY

May 2013

ABSTRACT

This thesis concerns the flashover issue of the substation insulators operating in a polluted environment. The outdoor insulation equipment used in the power delivery infrastructure encounter different types of pollutants due to varied environmental conditions. Various methods have been developed by manufacturers and researchers to mitigate the flashover problem. The application of Room Temperature Vulcanized (RTV) silicone rubber is one such favorable method as it can be applied over the already installed units. Field experience has already showed that the RTV silicone rubber coated insulators have a lower flashover probability than the uncoated insulators. The scope of this research is to quantify the improvement in the flashover performance.

Artificial contamination tests were carried on station post insulators for assessing their performance. A factorial experiment design was used to model the flashover performance. The formulation included the severity of contamination and leakage distance of the insulator samples. Regression analysis was used to develop a mathematical model from the data obtained from the experiments. The main conclusion drawn from the study is that the RTV coated insulators withstood much higher levels of contamination even when the coating had lost its hydrophobicity. This improvement in flashover performance was found to be in the range of 20-40%. A much better flashover performance was observed when the coating recovered its hydrophobicity. It was also seen that the adhesion of coating was excellent even after many tests which involved substantial discharge activity.

ACKNOWLEDGEMENTS

I would like to first and foremost offer my sincerest gratitude to my advisor, Dr. Ravi Gorur, whose encouragement, guidance and support from the initial to the final level enabled me to develop an understanding of the subject. I attribute the level of my Master's degree to his encouragement and effort and without him this thesis, too would not have been completed. One simply could not wish for a friendlier supervisor. I also want to express my gratitude to Dr. George Karady and Dr. Raja Ayyanar for their time and consideration in being a part of my graduate supervisory committee.

Financial assistance provided by the Power Systems Engineering Research Center (PSERC), a National Science Foundation Industry-University Cooperative Research Center, is greatly acknowledged.

I especially want to thank my parents Mr. Ujjiyel S. Gholap and Mrs. Vidya Gholap for the continual inspiration and motivation to pursue my utmost goals. I am deeply indebted to my brother for his love and understanding. I also would like to thank my friends and roommates who stood beside me and encouraged me constantly.

TABLE OF CONTENTS

Page

Page

LIST OF TABLES

Table Page

LIST OF FIGURES

Figure Page

NOMENCLATURE

^0C	Degree Celsius
A	Ampere
AC	Alternating Current
ASU	Arizona State University
ATH	Alumina Tri-hydrate filler
B	Exponent
CFO	Critical Flashover Voltage
CIGRE	International Council for Large Electric Systems
DF	Degrees of freedom
E	Energy
EPRI	Electric Power Research Institute
ESDD	Equivalent Salt Deposit Density
F	Standard “F” Statistic
FOV	Flashover voltage
FTIR	Fourier Transform Infrared
HC	Hydrophobicity Classification
HLD	High leakage distance
HVDC	High Voltage Direct Current
IEC	International Electrotechnical Commission
IEEE	Institute for Electrical and Electrical Engineers
I_r	Leakage current

K	Constant
L	Leakage Length
LD	Leakage Distance
LMW	Low molecular weight
MS	Mean sum of squares
NSDD	Non Soluble Deposit Density
P	Probability of testing the significance of null hypothesis
PDMS	Poly-di-methyl-siloxane
PRESS	Prediction error sum of squares
r_c	Per unit resistance of the polluted surface
R-Sq	Residual sum of squares
R-Sq (adj)	Adjusted residual sum of squares
R-Sq(pred)	Predicted residual sum of squares
RTV	Room Temperature Vulcanized
SD	Standard deviation
S_a	Salinity
SDG&E	San Diego Gas and Electric
SE Coef	Standard Error Coefficient
SPS	Site pollution severity
SS	Sum of Squares
STRI	Swedish Technical Research Institute
T	Standard “T” Statistic

UV	Ultraviolet
V	Volume
V_a	Arc voltage
V_r	Reignition voltage
V_s	Supply Voltage
x	Arc length
y	Response variable
z	Regressor function
β	Regression coefficient
ε	Error Term
θ	Temperature
μm	Micrometer
σ	Layer conductivity

Chapter 1. Introduction

1.1 Overview

The power system is a highly complex organization comprising of various entities aimed at delivering a reliable service to the end user. The power infrastructure includes a multitude of equipment such as generators, transformers, overhead transmission lines, transmission towers and insulators. Power generated at the stations is dispatched via a transmission network spanning thousands of miles. The conductors carry large amounts of power at high voltages typically more than 50 kV. Depending on the aesthetic purposes and cost, the cables can be placed overhead or laid underground. The overhead transmission lines are supported by the transmission tower which is a lattice structure made from steel. The conductor is separated from the metal part of the tower via an insulator assembly which comprises of an elongated body of electrically insulating material with metal end fittings. This arrangement ensures an air gap between line and tower or line and ground for a safe operation. In order to obtain a reliable power delivery it is paramount to maintain the mechanical stability as well as insulation in the network. High voltage outdoor insulators are therefore an indispensable part of the transmission network. The measure of reliability depends highly on the mechanical and electrical performance of the insulators used in the electric grid. Principal causes of insulator failures are punctures, vandalism, switching or lightning transients and pollution. These failures cause losses to the utilities and also reduce the reliability of the network.

1.2 Contamination flashover issue in transmission systems

The term flashover is defined as an unintended disruptive electric discharge over and around the insulator [1]. Contamination flashovers on transmission systems are initiated by airborne particles deposited on the insulator surface. These particles are due to industrial, construction or agricultural activities. The most commonly occurring pollutant is salt, which is a problem in coastal areas as well as inland areas where salt is used on roadways during winters [2]. The pollutants alone do not reduce the insulation strength in dry conditions. It is the presence of moisture combined with the deposits increases the risk of failure. Flashovers therefore occur in wet weather conditions, such as dew, fog or drizzle.

Primarily, the nature of the contaminants can be classified into two types namely soluble and non-soluble. The insulators installed near the vicinity of a coast are contaminated by soluble contaminants. Insulators that are near the vicinity of a construction site, cement or paper industries have non-soluble contaminants deposited on their surface. The soluble contaminants are expressed in terms of Equivalent Salt Deposit Density (ESDD) which corresponds to milligrams (mg) of NaCl per unit surface area of the insulator. In similar terms, the non-soluble contaminants are quantified in terms of Non-Soluble Deposit Density (NSDD), which correlates to mg of kaolin per unit surface area of the insulator.

Contamination based flashovers is one of the major causes of system outages in global utility network operations today as they are followed by a second flashover within in a short time. In case of multiple or successive flashovers, the utility needs to de-

energize the line and reclose it only after the surface is cleaned or in worst cases replace the insulator [2]. Historical data suggest that as early as 1902, wet flashover accident occurred on a high voltage line along the coast of Britain. In 1961, Japan alone had 162 flashover incidents due to pollution [3]. A survey conducted by the IEEE Working Group across North America in 1970 reported 306 specific case histories regarding the insulator contamination problem. The report revealed that the majority of cases lied in the voltage range from 69 to 138 kV [4]. Figure 1.1 shows a tabulated report of the cases from the IEEE Working Group Survey due to type of contaminant, weather and atmospheric conditions at time of trouble. The tabulated data shows that the maximum numbers of insulator failures occur in wet conditions in addition to the sea salt.

Contaminant type	Fog	Dew	Drizzle, mist	Ice	Rain	No wind	High wind	Wet snow	Fair
Sea Salt	14	11	22	1	12	3	12	3	-
Cement	12	10	16	2	11	4	1	4	-
Fertilizer	7	5	8	-	1	1	-	4	-
Fly ash	11	6	19	1	6	3	1	3	1
Road Salt	8	2	6	-	4	2	-	6	-
Potash	3	-	3	-	-	-	-	-	-
Cooling tower	2	2	2	-	2	-	-	-	-
Chemicals	9	5	7	1	1	-	-	1	1
Gypsum	2	1	2	-	2	-	-	2	-
Mixed contamination	32	19	37	-	13	1	-	1	-
Limestone	2	1	2	-	4	-	2	2	-
Phosphate and sulfate	4	1	4	-	3	-	-	-	-
Paint	1	-	1	-	-	1	-	-	-
Paper mill	2	2	4	-	2	-	-	1	-
Dried milk	1	1	1	-	-	1	-	1	-
Acid exhaust	2	-	3	-	-	-	-	-	-
Bird droppings	2	2	3	-	1	2	-	-	2
Zinc Industry	2	1	2	-	1	-	-	1	-
Carbon	5	4	5	-	-	4	3	3	-
Soap	2	2	1	-	-	1	-	-	-
Steel works	6	5	3	2	2	-	-	1	-
Carbide residue	2	1	1	1	-	-	-	1	-
Sulfur	3	2	2	-	-	1	-	1	-
Copper and nickel salt	2	2	2	-	-	2	-	1	-
Wood fiber	1	1	1	-	1	-	-	1	-
Bulldozing dust	2	1	1	-	-	-	-	-	-
Aluminum plant	2	2	1	-	1	-	-	-	-
Sodium plant	1	-	1	-	-	-	-	-	-
Active dump	1	1	1	-	-	-	-	-	-
Rock crusher	3	3	5	-	1	-	-	-	-
Total	146	93	166	8	68	26	19	37	4
% weather	25.75	16.4	29.3	1.4	12	4.58	3.35	6.52	0.71

Figure 1.1 Statistical data obtained for the type of contaminant, weather atmospheric conditions by IEEE Working Group [4]

Utilities employ various expensive mitigation techniques available to handle the contamination flashover problem. Cost optimization of insulation structures has always been the goal of the industry; therefore an optimum insulation level for a given system needs to be reliably determined. Therefore, considerable research therefore needs to be done to study the impact of the surrounding environment on the insulator performance to ensure an uninterrupted power supply.

1.3 Evolution of insulators

In simple terms, an insulator is “poor conductor” i.e. it has high electrical resistance. The primary function of an insulator is to provide a flexible or rigid support to the conductors or equipment and to insulate the conductors or equipment from ground or from other components or equipment [5]. It maintains an air gap for separating the line from ground. The length of the air gap depends on the system voltage, desired safety margin, on-site pollution level etc. Commonly used outdoor insulators have ceramic, glass or polymer as a dielectric medium. Figure 1.2 shows the types of insulators currently employed in the power infrastructure.

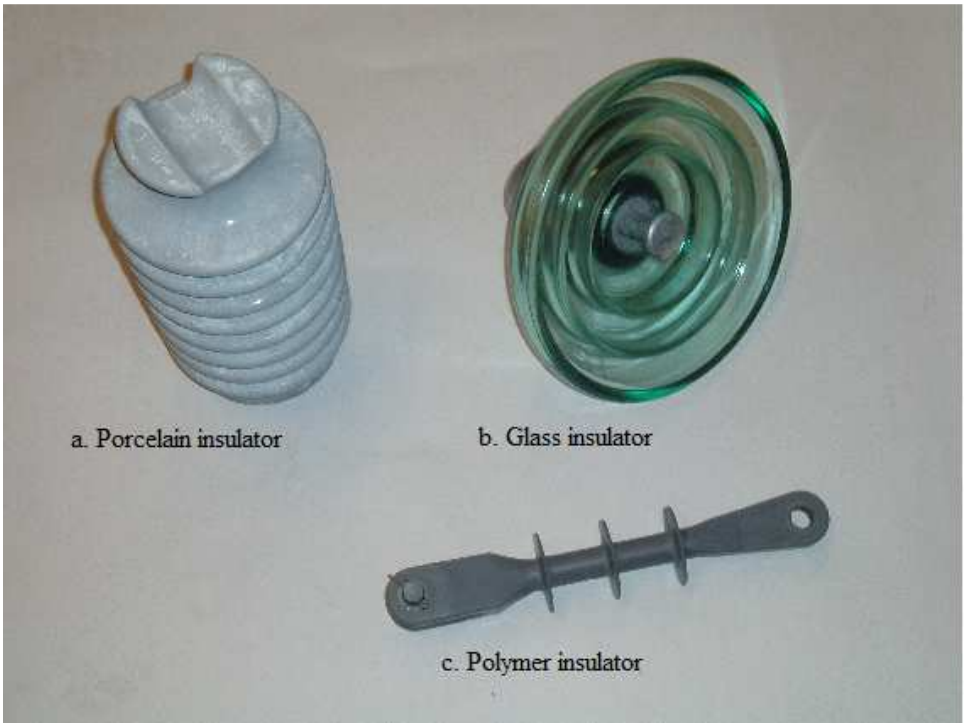

Figure 1.2 Types of insulator currently in use

Ceramic insulators have been used since the 19th century and have shown good reliability over the years. Glass and porcelain insulators were the only type available before

the introduction of composite insulators till the second half of the 20th century [6]. Since the 1960's, polymer or composite insulators have been preferred over the ceramic by many utilities for insulation. This switch was not because of the failure of ceramic insulators, but other benefits such as weight reduction by almost 90%, higher pollution performance and usage economy. The field performance for both classes of insulators, viz. ceramic and composite differs greatly due to the material properties. The Table 1.1 shows comparison between ceramic and polymer insulators [7].

Table 1.1 Comparison of Ceramic and Polymer insulation

Ceramic	**Polymer**
Material very resistant to UV, contaminant degradation, electric field degradation.	Material has good hydrophobicity but susceptible to degradation.
Strong under compression, weaker under tension.	Strong under tension but weaker under compression.
Modulus of elasticity is high i.e. the material is stiff.	The material is not stiff compared to porcelain.
Ceramic insulators are brittle and therefore require careful handling techniques.	The material is light and shock resistant in weight and easy to handle.
Low anti-tracking and erosion resistance.	Excellent tracking resistance.

The most important property which differentiates the aforementioned materials used in insulators is the surface free energy. In simple terms, surface free energy can be defined as the energy associated with the intermolecular forces at the interface between two media. Ceramic insulators have high surface free energy which results in greater adhesion to water and are therefore highly wettable. This property of high wettability is not desirable for an insulator operating in a polluted environment. Water along with pollutants ac-

cumulated on the surface form a conducting layer which allows the flow of a leakage current affecting its flashover performance.

Polymers used in composite insulators have low surface free energy and hence have good hydrophobicity. The polymeric material inhibits the formation of a continuous water film and therefore suppresses the leakage current thereby improving its contamination flashover performance. In recent years, silicone water-repellent coatings have attracted considerable interest for improving the pollution based flashover performance.

The liquid silicone Room Temperature Vulcanized (RTV) coating has gained considerable popularity since the first field trial in 1973 with an experimental product and the first large scale application in 1987 with a commercial product [8]. These coatings have been used on post insulators and large diameter porcelain bushings and have been effective under conditions of light pollution. Successful applications of these coatings at various HVDC converter stations such as Nelson River and Sylmar have established the strong ability of the coating to suppress the leakage current [9]. However, there is limited knowledge available on the long term performance of these polymeric coatings in presence of various environmental stresses. Therefore, there is a need to study the ageing characteristics which these coatings undergo and to the ageing of the insulator performance [10].

1.4 RTV Silicone Rubber Coatings

The commercial RTV coatings consist of a poly-di-methylsiloxane (PDMS) polymer, reinforcing filler such as fumed silica, alumina tri-hydrate filler, a colorant pigment, and a cross-linking agent. The coating may also contain PDMS fluid, additional

fillers, a condensation catalyst, and an adhesion promoter for improved bonding to ceramic surfaces. The properties of adhesion to surface of porcelain, hydrophobicity and the ability to suppress the leakage current are highly important for evaluating the on-field performance of the coatings. These properties depend on the amount and type of ATH and other fillers, the degree of cross-linkage, the adhesion promotion, and the amount of free fluid [8]. The ability of the coating to maintain its hydrophobicity is highly attributed to the chemical stability and hydrophobicity recovery phenomenon caused by the diffusion of low molecular weight (LMW) polymers. Prolonged wetting gradually removes the free silicone free fluid from the surface and the coating loses its non-wettability property and therefore the ability of suppressing the leakage current. However during dry period the free fluid migrates to the surface and restores hydrophobicity. The studies on suppression ability of RTV coatings on leakage current involve testing in salt-fog chamber or a tracking wheel. Figure 1.3 indicates the loss of hydrophobicity of an RTV coated insulator due to prolonged wetting in a salt-fog test [8].

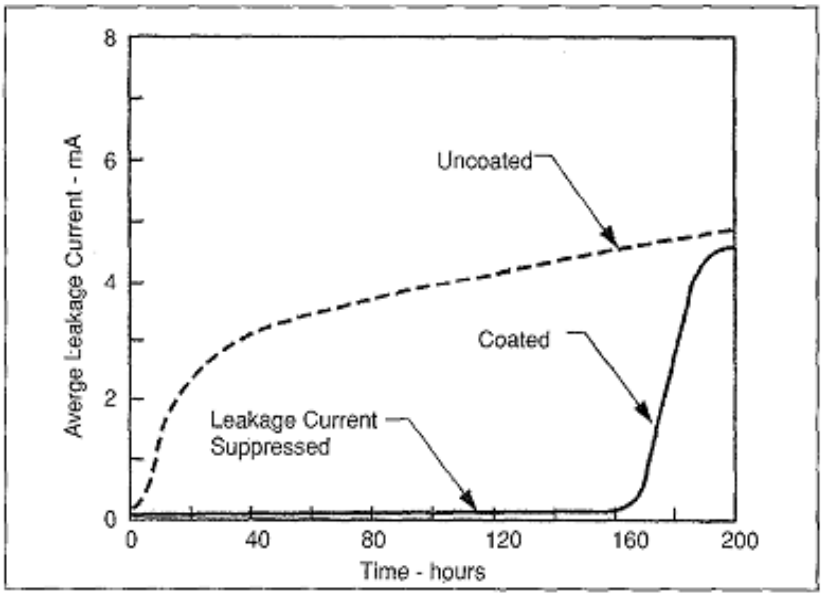

Figure 1.3 Suppression of leakage current on a coated insulator tested in a fog chamber

1.5 The Coating Concept:

Porcelain insulator constitutes about 65 % of the power market in the transmission system [6]. Utilities primarily use the outdoor apparatus porcelain insulators to support rigid bus connections and other electrical equipment. Various maintenance practices are followed by the utilities to prevent disruptions in the grid due to contamination flashover [11]. Common practices include regular cleaning of the insulator surface or increasing leakage distance. Maintaining a cleaning schedule is expensive and time consuming. A less expensive way is to increase the leakage distance by using an additional insulator or by replacing the contaminated insulator by a larger unit. This method has its own limitations and is not used very often. Other techniques include application of silicone and petroleum grease on the insulator surface. However, the grease coatings tend to lose their water repellency when exposed to ultraviolet (UV) light or heavy contamination.

Coating the porcelain insulator with silicone rubber is one way to improve the water repellency of the surface to avoid flashover. The coating can be applied to the surface by spraying, painting or dipping the liquid polymer, which then vulcanizes in presence of air into a flexible rubber layer. This concept of coating the porcelain insulator for protection is relatively new but has instilled considerable interest as a maintenance technique [11].

1.6 Motivation

The utilities are able to select the insulator type according to the system and design requirements. In order to improve the contamination performance, they need to opt for high leakage porcelain (HLD) units, which can be taller or have wider sheds than standard porcelain units. However, for an optimal design of substation insulation it is desirable to improve the contamination flashover without increasing the height or width of the unit.

RTV silicone rubber coated insulators is a practical option for improving flashover performance in presence of pollution without compromising on the mechanical aspects of the substation design. The motivation of this study is to compare the performance of bare and RTV silicone rubber coated insulators by performing fog chamber tests in the laboratory. Overall assessment of several important aspects of the coating such as adhesion to porcelain, hydrophobicity, contamination flashover and weathering is provided in the study. A good statistical model predicting the flashover will be a desirable asset to the utilities, helping to improve substation design in the future. The study aims to build a comprehensive model for predicting the flashover performance of the

RTV silicone rubber coated insulators. Regression analysis technique is used for model building in this work.

1.7 Organization of thesis

The thesis is divided into five chapters. The chapter 2 gives the literature review of the models developed by earlier researchers. Chapter 3 provides an introduction to the concepts in design of engineering experiments and regression analysis. The research work is described chapters 4 and 5. Chapter 4 gives the details of the experiments and the samples employed in the study whereas, chapter 5 provides the results and analysis of the experimental findings. The conclusions and future work is provided in chapter 6.

Chapter 2. Literature Review

2.1. Introduction

This chapter provides an overview of the contamination problem of the insulators and flashover theory. Theoretical models proposed by various researchers are also discussed in detail. Various researchers have developed prediction models for contamination flashover using regression analysis techniques. A brief introduction to the regression technique is also provided in this chapter.

2.2. Pollution: Definition

"*Pollution can be defined as the introduction of substances or energy into the environment that can endanger human health, harms living resources and ecosystems, or impairs assets"*. Electric substation and line equipment located in the outdoor environment have a wide range of problems associated with pollution. Predominantly, the insulators undergo accelerated corrosion damage, a high rate of buildup of surface pollution and heavy localized wetting in moist conditions [12]. According to the report of an IEE-EEI joint committee in 1966, insulator contamination is the second major cause of transmission line outages [2].

Typical pollution environment are marine, industrial, agricultural and desert. They are defined in the CIGRE Task Force 33.04.01 as follows.

- Marine environment, where proximity of the sea introduce Na, Cl, Mg, K and other marine salts into the atmosphere.
- Industrial environment include sources of soluble pollution from steel mills, refineries or sources of dust such as quarries and cement factories.
- Agricultural environment includes pollutants from highly soluble fertilizers as well as insoluble dust and chaff.
- Desert environment introduces pollutants like inert sand as well as salt in some areas.

The utilities use various methods for monitoring the on-site pollution on insulator units. Table 2.1 shows utility practices for assessing pollution severity [12].

Table 2.1 Pollution severity monitoring practices

Method used	**Measured Parameters**
Insulator leakage current online monitoring	Current (mA)
Air quality on-line monitoring	Particulate concentration (eg., $PM_{2.5}$)
Daily contamination monitoring of chilled insulator samples	Insulator leakage resistance(Ω) or surface resistance(Ω)
Daily visual inspection of insulators	Light transmission level, color
Hydrophobicity inspection	Visual hydrophobicity classification guide (HC0-HC6)
Equivalent salt deposit and non-soluble deposit density measurements	Contaminant amount per unit surface area (mg/cm^2)
Annual or long term flashover frequency	Flashovers per 100 km of line length per year

The above mentioned methods contribute to

- Determine the site pollution severity (SPS) which is useful for improving the design for reliable electrical performance.
- Take appropriate measures to avoid damage by scheduling maintenance operations.
- Quantifying the performance of different insulators for comparison in different laboratory testing conditions.

2.3. Measurement and levels of pollution severity

The pollution severity of a location is quantified in terms of Equivalent Salt Deposit Density (ESDD). It is defined as the *quantity of sodium chloride (NaCl) per unit area sampled which gives the same conductivity of that of the deposit removed* [13]. The ESDD value provides a classification of the pollution severity in the zone, considers the weather factors like humidity, pressure, rain and wind velocity. It is expressed in units of mg or µg of NaCl per cm^2 of surface area. According to IEC Standard 60815, 1986 values of 10 µg/cm^2 are considered light, while values above 400 µg/cm^2 are very heavy. Table 2.2 as shown below gives the range for the ESDD for various pollution levels [14].

Table 2.2 ESDD values as per IEC 60815

Class	**ESDD**	**Pollution Level**
I	0.03-0.06	Light
II	0.1-0.2	Medium
III	0.3-0.6	Heavy
IV	0.6	Very heavy

2.4. Hydrophobicity classification

The electrical performance of the polymer insulators depends on the hydrophobicity i.e. the water-repellency of the surface. The hydrophobicity however will change with time due to exposure to the outdoor environment and partial discharges [15]. Ceramic surface is however easily wettable which endangers the performance in highly polluted conditions.

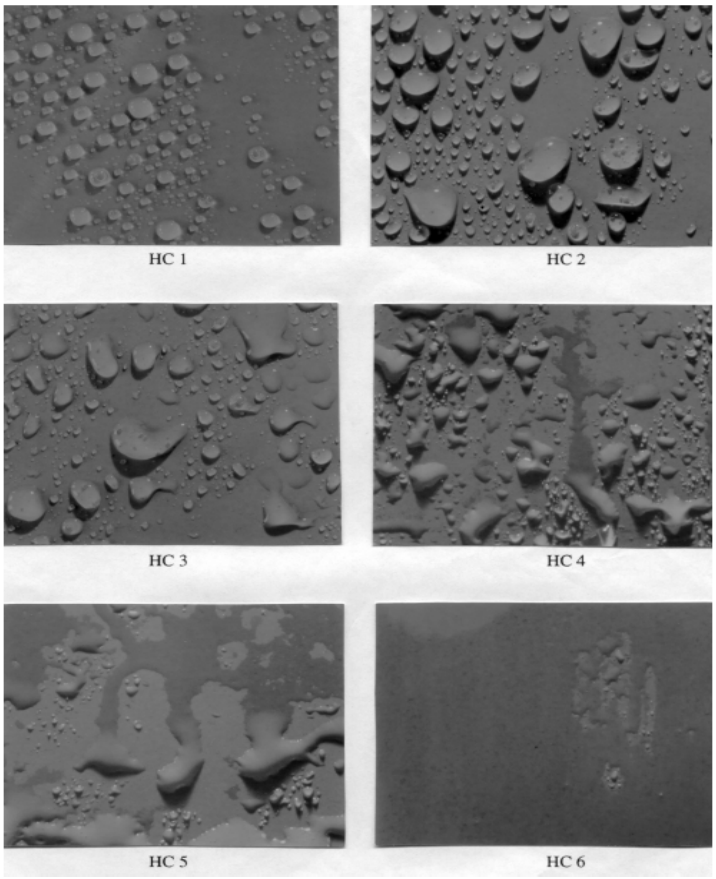

Figure 2.1 Hydrophobicity classification STRI 92/1

Seven classes of hydrophobicity (HC 1 – HC 7) have been defined as shown in Figure 2.1. HC – 1 corresponds to a completely hydrophobic surface and HC – 7 to a

completely hydrophilic surface. This method is fast and an easy way to check the wetting status of the insulators in the field.

2.5. Flashover Theory: Breakdown of polluted insulators

The electrical performance of polluted insulator depends on the wettability of the surface. Porcelain being hydrophilic, conducts a large leakage current than the hydrophobic polymer material. The wettability property of the material gives rise to different modes of breakdown ultimately leading to flashover. The two different modes for breakdown in hydrophilic and hydrophobic materials are explained as follows.

Contaminated Hydrophilic Surface

The flashover on the polluted hydrophilic surface involves the following sequence of events [16].

1. Pollution layer forms on the surface due to external environment. The dry pollution layer has high resistivity and therefore does not affect the electrical performance
2. The wetting of pollution layer takes place in atmospheric conditions such as fog, dew, drizzle, rain, snow or ice. The wetting results in formation of an electrolyte layer which conducts measurable leakage current on the surface of the insulator.
3. The flow of leakage current leads to spots with higher current density. This causes high localized heating and therefore results in evaporation of the moisture leaving the surface with a dry spot. Many dry spots may spread and coalesce to form a single dry band.

4. A concentration of voltage stress is formed around the dry band as its conductivity is very low. This is because of the fact that almost all the voltage applied is across the dry band. If the electric field is high enough, a breakdown of air will occur resulting in formation of a local arc.
5. The dry band will grow as a result of heating near the arc roots. The local arc may move laterally to an area with higher field stress or along the electrolytic surface eventually causing a flashover.

Contaminated Hydrophobic Surface

The hydrophobic insulators do not get wet completely. Therefore, breakdown mechanism is more complex over a hydrophobic surface.

1. Water droplets are formed initially due to environmental wetting. The pollution diffuses through the thin layer of surface oil and dissolves in the water droplets to form a conductive spot on the surface. Several spots coalesce and leakage currents start to flow.
2. The heat developed due to the high current density dries up some wet areas and an equilibrium is reached between evaporation and wetting. Low conductivity of the polymer surface persists between wet areas.
3. The interaction between the electric field and droplets tend to elongate the wet areas into filaments [17].
4. Field intensification at the tips of the filament produces spot discharges that are randomly distributed across the surface.
5. The surface discharges erode the hydrophobicity leading to irregular wetted areas.

6. Finally a combination of filament growth and wet areas eventually short out a conductive path for the arc causing flashover.

2.6. Review of Flashover Models

Many researchers have worked and published papers on the flashover modeling subject in the last 70 years. It is important to note that a large amount of recent publications are based on classical model developed by Obenaus. This section provides a review of theoretical as well as statistical models developed over the years.

DC Models

Obenaus initiated the theoretical study of flashover of polluted insulators [18]. He outlined the steps to determine the flashover voltage using the concepts of surface resistance of polluted layer and dry band formation. Neumarker, further developed the idea assuming a uniform pollution resistance per unit length for the pollution layer. However, in practice the pollution distribution is non-uniform. Moreover, a practical scenario consists of non-uniform wetting and drying leading to multiple dry band formation. For simplification, the assumptions that the model incorporates are: Single dominant arc, uniform pollution distribution and uniform wetting [19]. In his theory, Obenaus modeled the flashover process as a discharge in series with resistance as shown in Figure 2.2.

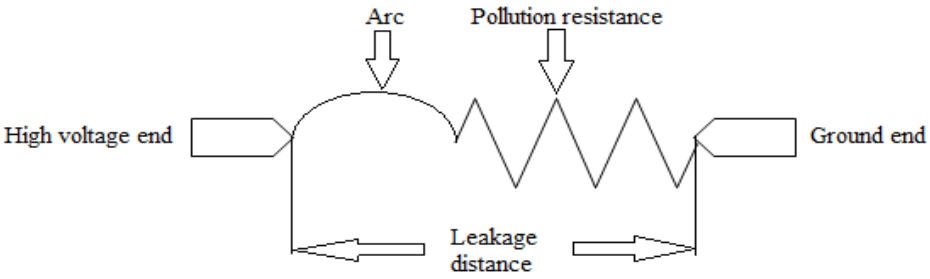

Figure 2.2 Obenaus model for polluted insulator

The discharge represents the dry band arc and the resistance, the pollution layer of the unabridged portion. The equation for the above circuit is written as

$$V_s = V_a + R(x) * I \qquad 2.1$$

Where,

V_s: Supply voltage in Volts

V_a: Arc voltage in Volts

$R(x)$: The resistance from grounding electrode to the arc root in Ω

I: The leakage current in A

The arc voltage V_a is given by the following relationship

$$V_a = AxI^{-n} \qquad 2.2$$

Where

A, n: Arc constants

x: Length of the arc

Alston and Zoledziowski developed a simplified model by considering simple cylindrical insulator geometry. They further developed the Obenaus model using $V_s = A * x * i^{-n} + i * R$; the assumption made was that if the length of the polluted discharge-free

area were great compared with the diameter of the cylinder, the electric field would be uniform over the greater part of the length. Therefore a linear relationship for the pollution resistance is obtained as given below [20],

$$R = r_c * (L - x) \tag{2.3}$$

Where,

R : Resistance

r_c: Per unit resistance of the polluted surface

L: Leakage length

x: Length of the arc

Further analysis of the model led to important conditions at which the arc extinguishes. The voltage required to sustain the local discharges on polluted insulators may increase with an increase in the discharge length [1]. This happens at a particular voltage for a given length of the arc. The relationship obtained is as follows

$$V_c = A^{1/(n+1)} * L * r_c^{n/(n+1)} \tag{2.4}$$

Where

V_c: Critical voltage at which the arc extinguishes

And the critical length of the arc is given by the expression as follows

$$x_c = L/(1 + n) \tag{2.5}$$

The critical value of the current (i_c) is calculated as [20]

$$i_c = \left(\frac{A}{r_c}\right)^{1/(n+1)} \tag{2.6}$$

Hampton proposed a criterion for the propagation of arc based on the polluted strip and water jet experiments. The experiments studied the formation of dry bands and

the subsequent growth of discharges on the polluted surface of a strip by scanning the voltage distribution at high speed [21]. Based on the measurements of the voltage distribution, it was concluded that for an arc to propagate over a resistive surface, the voltage gradient on the surface must exceed the voltage gradient in the arc column.

A dynamic model to study the dc flashover by taking into account the insulator profile was developed by R. Sundararajan. The model incorporated Obenaus' and Neumarker' theory as well as Hampton' arc propagation criteria. The pollution resistance was varied by calculating the form factor at every instant as the arc propagated [19]. The dynamic change in arc resistance as the arc traverse along the leakage path was used to compute the flashover voltage in the new model. A better correlation between the values obtained from the model with the experimental data was achieved.

AC Models

The above DC model can also be applied for an AC flashover phenomenon. However the constants A and n values are different from those of a DC flashover model. Alston obtained values for A, n to be 63 and 0.76 from the curve fitting for a DC model [20]. However for the same model with an AC energization, Woodson used A to be 200 and n to be 6.3.

Claverie established relations between voltage, current and arc length from an electrical circuit composed of an AC arc in series with a resistance. The model incorporated arc reignition conditions. The relationship for the minimum voltage supply that is needed to ensure reignition of an AC arc from the previous half cycle is given by [22, 23],

$$V_r = AxI_r^{-n} \quad 2.7$$

V_r: Reignition voltage

A: Arc reignition constant

x: Arc length (mm)

n: Arc reignition exponent

I_r: Peak value of the leakage current in previous half cycle (A)

The above equation is similar to equation 2. Similar equations for critical arc length (x_c), critical stress (V_c) and critical current (i_c) can be obtained.

Regression Models

Statistical techniques are particularly used in modeling and ageing studies in insulation field. Based on field experience, good theoretical models have been developed for predicting the flashover performance of ceramic insulator. However, not much work has been done in flashover performance of the non-ceramic insulators. Non ceramic insulators offer challenges such as different modes of surface dynamics and ageing. Using regression techniques, it is possible to incorporate the factors such as hydrophobicity, ageing and contamination accumulation in modeling the flashover performance of the non-ceramic insulators. S.Venkataraman estimated the flashover performance of insulators under contaminated conditions using a combination of experiments and regression analysis [1]. The models developed in the study represented a generic form of a regression line given as follows.

$$y = \beta_0 + \beta_1 x + \varepsilon \quad 2.8$$

Where

y: Response variable (flashover voltage)

β_0: Intercept

β_1: Slope

x: Regressor or predictor variable (esdd, leakage distance or surface resistance)

ε: Error term

The contamination severity expressed in terms of ESDD, surface resistance and leakage length represented the regressor variables in Venkatraman' model. In 1988, researchers at EPRI High Voltage Transmission Research Center developed regression models to capture the effect of shed configuration on the contamination performance of post insulators for HVDC converter stations. The study was based on artificial contamination tests carried out on twelve different post type insulators by various manufacturers. The model related the voltage corresponding to fifty percent probability of flashover, or critical flashover voltage (CFO) to the contamination severity in terms of esdd and is given as following [13],

$$\mathrm{CFO} = \mathrm{K}(\mathrm{ESDD})^{-\mathrm{B}} \qquad 2.9$$

R. Sundarajan also developed a dynamic model for insulators energized with dc voltage on similar terms. The general findings from the work are as shown below [24]

$$FOV = K(ESDD)^{-0.33} \quad 2.10$$

$$FOV = k(LD)^{n} \quad 2.11$$

Where,

FOV: Flashover Voltage in kV; n: Leakage distance exponent ; K, k: Constants

ESDD: Equivalent Slat Deposit Density in mg/cm^2 ; LD: Leakage distance in cm

Similar values were obtained for the ESDD exponents in the models by EPRI and Sundararajan.

Chapter 3. Introduction to Designed Experiments and Regression Analysis

This research focuses on building a model using the experimental data obtained from the surface resistance measurement and flashover tests. It is therefore customary to plan the experiments so that the analysis of the resulting data is capable of providing valid and objective conclusions. This section provides the basics of the design of experiments and regression techniques.

3.1 Design of Experiments

Formally, an experiment can be defined as *a test or series of tests in which purposeful changes are made to the input variables of a process or system so that the observer may observe and identify the reasons for changes that may be observed in the output response* [25]. In any scientific inquiry, experimentation is a vital part. In certain situations, the scientific phenomena for a process are well understood and mathematical models can be developed directly from the physical mechanism. Such models are known as mechanistic models. However, most engineering problems require observation of the system and experimentation to interpret the behavior. In such cases, well designed experiments can lead to an empirical model.

Designed experiments primarily employ statistical techniques to study the influence of a factor or factors (input variables) on a response (output) in a process. In an experiment, the independent variable is known as a factor and can be manipulated by the experimenter. In engineering, it is common to have more than one factor to be included in the study. The correct way to study multiple factors is to conduct a factorial experiment in which the factors are varied together, instead of one at time. In other words, in each com-

plete trial or replication of the experiment all possible combinations of the levels of the factors are investigated in a factorial design. Most frequently used designs are two level factorial designs[25].

A general two-level factorial design can be represented as 2^k design, where k is the number of factors in the experiment each at two levels (i.e. two different values of the factor). The levels of the factor can be quantitative, representing the physical properties such as temperature, velocity; or they can also be qualitative, such as two machines or two operators. Another common type of design encountered in the experimentation is the 3^k design. This design has a factorial arrangement with k factors at three levels. Similar to the nature of factor levels in a 2^k design, the factors in a 3^k design can be quantitative or qualitative [25]. In this study a 3^2 design is employed for modeling the behavior of contamination flashover. The ESDD levels (contamination severity) and leakage length are the two factors considered. Each of the factors is at three different levels. The design is explained in chapter 4.

3.2 Regression Analysis

Regression Analysis is a statistical technique for investigating and modeling the relationship between variables [26]. The dependent variable is known as the response and the explanatory or independent variables are referred to as predictors. Regression analysis helps to understand the effect on the dependent variable when one of the independent variables is changed while the other independent variables are fixed. The equation obtained by applying the technique is an approximation to the true functional relationship between the variables of interest. Depending upon the nature or mechanism of the functional relationship between the dependent and independent variables, the regression models are classified as

1. Linear regression model
2. Non-linear regression model

Linear regression model

A relationship between the response and a regressor of the form of a straight line is characterized as a linear regression model. The response y is related the regressor x as shown below.

$$y = \beta_0 + \beta_1 x + \varepsilon \qquad 3.1$$

Where

β_0: intercept

β_1: Slope

ε: Error term

The above model has only one predictor variable. However, in many practical cases it is possible to have more than one variable. Such a model is known as multiple linear regression model.

The multiple linear regression model is of the form

$$y = \beta_0 + \beta_1 x_1 + \beta_2 x_2 + \cdots + \beta_k x_k + \varepsilon \qquad 3.2$$

Where

$x' = [1, x_1, x_2, \ldots, x_k]$

The above model as shown in equation 13 is capable of including polynomial models as well as other complex relationships in addition to first order relationships. In such cases the regression equation can be modified as shown below,

$$y = \beta_0 + \beta_1 z_1 + \beta_2 z_2 \ldots . + \beta_k z_k + \varepsilon \qquad 3.3$$

Where z_i represents any function of the original regressors $x_1, x_{2,} \ldots , x_{k.}$

The above model in equation 14 is also considered as a linear model as it is linear in the unknown parameters

Therefore in a more general form, the linear regression equation can be written as

$$y = x'\beta + \varepsilon$$
$$y = f(x, \beta) + \varepsilon \qquad 3.4$$

Linear regression models are popular among the analysts as they are simple and provide a flexible framework for analysis. However, they may not be appropriate in all situations. Many problems in engineering have a response related to a variable or variables through a non-linear function [26]. Any model that is not linear in the unknown parameters is a nonlinear regression model. It is of the form as shown below.

$$y = f(x, \theta) + \varepsilon \quad 3.5$$

Where

θ: p x 1 vector of unknown parameters

ε: Random error term

In this work, a model as given by equation 15 is used to develop a prediction model.

The basic assumptions linear regression models include for purposes of prediction are as follows [27]:

- Linear relationship between dependent and independent variables
- No correlation between the errors
- Constant variance of the errors versus time or predictions
- Normal error distribution

Finally, it is important to note that regression analysis is a part of a broader data analytic approach to problem solving. Generally, it is important to have insight and understanding of the system under study. A good data collection scheme and a strong model adequacy check in addition to the knowledge of the process lead to a resourceful model.

Chapter 4. Evaluation of insulator samples

4.1 Introduction

This chapter gives an overview of the sample preparation technique and testing methods employed to evaluate the performance of the insulators. The procedure for artificial contamination is also described.

Twelve 69 kV post-type porcelain insulator samples were provided by San Diego Gas and Electric Company (SDG&E Co.) Initial inspection of the samples did not reveal any damage or anomaly in the samples. Eleven samples were coated with RTV Silicone Rubber coating by a private contractor provided by SDG&E Co. The coating was applied in a dust-free spray booth facility available at the Arizona State University (ASU) Campus. After the coating was applied, the samples were left to dry for one day before subjecting to any laboratory tests.

4.2 Samples evaluated

As mentioned, the samples for the study included one porcelain post type insulator and seven RTV silicone rubber coated insulators. The samples were subjected to artificial contamination tests after the initial inspection. These tests are intended to provide information on the behavior of external insulation under the conditions which represent the contamination encountered in the service. The tests may not necessarily simulate any particular service environment.

Table 4.1 Insulator samples used in the study

Sample Name	Surface material	Leakage distance (cm)	Nominal rating (kV)
P	Porcelain	183	69
N1	RTV Silicone Rubber	183	69
N2	RTV Silicone Rubber	183	69
N3	RTV Silicone Rubber	183	69
N4	RTV Silicone Rubber	183	69
N5	RTV Silicone Rubber	183	69
N6	RTV Silicone Rubber	183	69
N7	RTV Silicone Rubber	183	69

4.3 Artificial contamination of insulators

The pollution layer in the laboratory is achieved by artificial contamination method. Slurry prepared by mixing common salt (NaCl) and kaolin in water is applied on the insulator sheds to simulate coastal contamination. The proportion of salt and kaolin is varied to obtain different contamination levels.

The test object is carefully cleaned to remove all the traces of dirt. The contamination slurry is then applied to the insulator surface using a brush. The application of the slurry is repeated multiple times so that a uniform layer of pollution is achieved on the top as well as the bottom surface of the insulator sample. The sample was then allowed to dry. The drying period was about 10 hours before subjecting it to test under high voltage. After the insulator sample is dried, the ESDD level is measured. The technique used to measure ESDD level in the laboratory is known as the rag-wipe method. A clean cloth /

cotton is rinsed in a fixed volume of deionized water. A fixed area on the shed is wiped using the cloth / cotton. The cloth is then rinsed in the deionized water. The conductivity (σ_θ) of the rinsed solution is then measured using a Horiba conductivity meter at a temperature θ (^{0}C). Then the value of the conductivity of the rinsed solution at 20 ^{0}C is obtained by using the following equation.

$$\sigma_{20} = \sigma_\theta[1 - b(\theta - 20)] \quad 4.1$$

Where,

σ_{20}: Layer conductivity at a temperature of 20 ^{0}C in S/m

σ_θ: Layer conductivity at a temperature of θ^0C in S/m

b: Factor depending on the temperature as given in Table 4.2 as shown below

Table 4.2 b factor values at different temperatures

θ	b
5	0.03156
10	0.02817
20	0.02277
30	0.01905

The salinity S_a of the solution is then measured by using the formula,

$$S_a = (5.7\sigma_{20})^{1.03} \quad 4.2$$

The ESDD in mg/cm^2 is then obtained by the following formula

$$\text{ESDD} = S_a \frac{V}{A} \quad 4.3$$

Where,

V: Volume of the rinsed solution in ml

A: Area of the cleaned surface of the sample in cm^2

Every contaminating practice leads to some difference between the ESDD values measured on the top and bottom shed surfaces of the insulator sample. This difference is affected by both insulator shapes as well as the type of the slurry used for contamination. According to IEEE Std 4 for high voltage testing techniques the ratio between a local measurement of ESDD and that on the whole area of the insulator should lie in the interval 0.7-1.3 during the wetting in a fog chamber test [28].

4.4 Experimental setup

Primarily the experiments involved in this research are:

- Surface resistance measurement
- Flashover

The experiments were carried out for both types of samples i.e. porcelain and silicone rubber coated insulators. Fog chamber tests provide a comprehensive method for simulating different environments in a laboratory. The tests are categorized as follows

- The clean fog tests
- The salt fog tests

These tests involve application of contamination and the simultaneous or subsequent application of voltage. Clean fog tests were used for measuring the surface resistance and flashover tests in this research. In this test, the fog generators provide a uniform fog distribution over the length and around the test object. According to the IEEE Std 4 the temperature of the test object at the beginning of wetting should be within 2^0C of the ambient temperature in the test chamber [28].

Description of the fog chamber

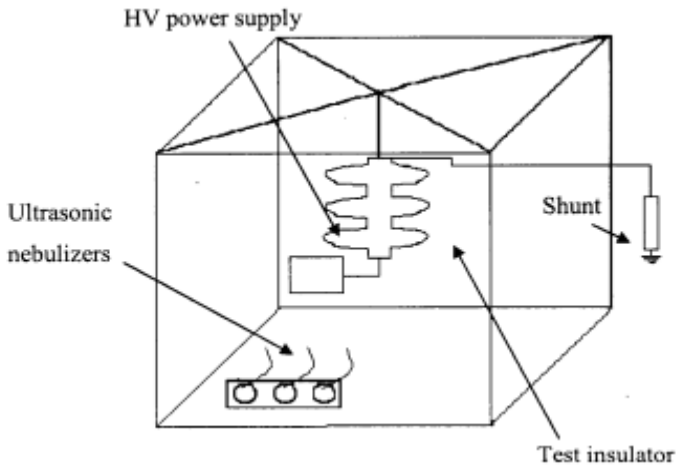

Figure 4.1 Schematic of the fog chamber

The fog chamber test facility available at ASU' High Voltage Laboratory is made of stainless steel sheets [1]. The dimensions of the chamber as shown in the Figure 4.1 are 3.66 m X 3.05 m X 2.44 m which makes it a volume of 27 m^3. A plexiglass window 30 cm X 20 cm is fitted on the stainless steel door for visual observation. High voltage is supplied by a transformer rated at 40 kVA/ 100 kV. The transformer is stationed outside the chamber and the connection inside the fog chamber is through a cable. Fog is generated by using four ultrasonic nebulizers placed in the water tub. The water droplets formed on the surface of the insulator due to the fog generated by ultrasonic nebulizers are typically 1µm in diameter [29]. A relative humidity level of 100% is achieved within 40 minutes after switching on the ultrasonic nebulizers.

Figure 4.2 Experimental set-up in the fog chamber

Procedure

The insulator sample is mounted vertically on the wooden platform inside the fog chamber as shown in Figure 4.2. It is placed in such a way that the source of fog is not directly beneath. Adhesive aluminum tape was used as a return electrode. The main electrode was connected directly to the metal cap using a bolt to ensure a tight electrical connection.

The ultrasonic nebulizers were switched on for generating the fog. After about 45 minutes an AC voltage is applied by switching on the power supply. The voltage applied depends on the dimensions of the insulator sample. The voltage applied ensured that a measurable leakage current was established. Also care was taken such that the voltage

applied was not high enough to initiate discharges. The voltage in the range of 2 kV – 6 kV was used to measure the surface resistance.

After the energization, the data acquisition system was switched on. An oscilloscope is used as a primary data acquisition system. The voltage drop signal is measured across the series resistance. The resistor box has three options of 100 Ω, 470 Ω and 1000 Ω for choosing an appropriate series resistance. The surface resistance is calculated by using Kirchhoff' voltage law i.e. the applied voltage is the sum of the voltage drops across the insulator sample and the series resistance. A new data acquisition developed using a DAQ device interfaced with Lab VIEW program was also used in addition to the oscilloscope. The program continuously monitors the leakage current signal during the test run, identifies any points in time the signal exceeds an established threshold of noise, and sorts the signals into data bins based on their peak magnitudes. Experiments were carried out using the above procedure to measure the surface resistance as well as to estimate the flashover voltage of the sample at various contamination levels. For measuring the flashover voltage, a voltage of about 80 % of the probable flashover voltage (from trials) is applied to the sample after a 100% humidity level is achieved in the chamber. If there is no flashover, then the voltage level is raised in steps of 2 kV and maintained for 5 minutes until the flashover is achieved. A set of three flashover readings were obtained in one experiment. The flashover voltage measured is the average of the three readings obtained [1].

Chapter 5. Experiment design and results

5.1 Description of the experiment design

As mentioned in Chapter 4, a factorial design was chosen to build the flashover prediction model. The response and factor variables considered in the experiment design are described as follows.

- Response variable: Flashover voltage (FOV) in kV
- Factor 1: Contamination severity (ESDD) in mg/cm^2
- Factor 2: Leakage length (LD) in cm
- Factor 3: Surface material (Porcelain or RTV Silicone Rubber)

Factor level determination

ESDD: The levels of ESDD were chosen such that the model is capable of predicting the flashover voltage from medium to very high level of pollution severity. The Zed curve [12] in Figure 5.1 shows the region of interest for the study.

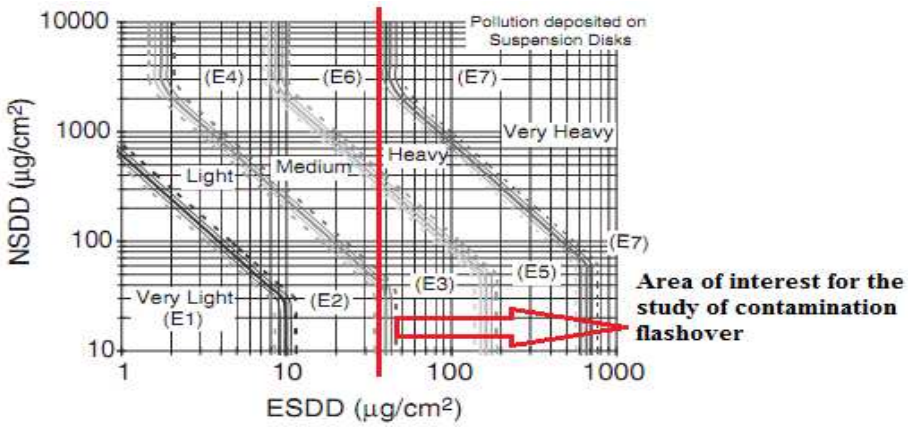

Figure 5.1 Zed curve approximation to IEC site pollution severity (SPS) guidelines

The ESDD levels set for the experiment vary from 0.1 mg/cm^2 to 0.5 mg/cm^2. A 0.1 mg/cm^2 corresponds to a low level of contamination while 0.5 mg/cm^2 corresponds to a very high level of contamination.

Leakage distance: The insulator samples provided by SDG&E were 69 kV NGK-Locke station post with a leakage distance of 183 cm. The leakage length was varied in the experiment such that it corresponds to the leakage distance of 23 kV and 46 kV insulators. Therefore, three different levels distance were considered in the experiment design.

Surface material: The type of the material is considered as a categorical variable. The types of surface material encountered are porcelain and RTV silicone rubber.

The design of the experiment was done using JMP Software. The runs obtained from JMP are shown below.

Table 5.1 Experimental Design

Leakage distance / **ESDD**	**61 cm**		**109 cm**		**183 cm**	
0.1 mg/cm^2	Porcelain	RTV	Porcelain	RTV	Porcelain	RTV
0.3 mg/cm^2	Porcelain	RTV	Porcelain	RTV	Porcelain	RTV
0.5 mg/cm^2	Porcelain	RTV	Porcelain	RTV	Porcelain	RTV

5.2 Experimental Results

Porcelain Insulators

The flashover experiments were carried out on a bare porcelain insulator sample by varying the leakage length and the levels of contamination. Following are the results from the flashover tests

Voltage Class: 23 kV

Table 5.2 Flashover voltages for 23 kV voltage class at different levels of ESDD

ESDD (mg/cm^2)	**Leakage distance (cm)**	**Flashover voltage (kV)**
0.12	61	21
0.13	61	20
0.31	61	17
0.33	61	16
0.51	61	13
0.49	61	15

Voltage Class: 46 kV

Table 5.3 Flashover voltages for 46 kV voltage class at different levels of ESDD

ESDD (mg/cm^2)	**Leakage distance (cm)**	**Flashover voltage (kV)**
0.107	109	38
0.115	109	36
0.32	109	25
0.3	109	28
0.52	109	20
0.507	109	23

Voltage Class: 69 kV

Table 5.4 Flashover voltages for 69 kV voltage class at different levels of ESDD

ESDD (mg/cm^2)	**Leakage distance (cm)**	**Flashover voltage (kV)**
0.13	183	38
0.12	183	36
0.33	183	25
0.31	183	28
0.5	183	20
0.51	183	23

A regression based model was developed using the above flashover data. Minitab 16 was used for all the statistical analysis.

Regression Analysis: Porcelain insulator model

The response and predictor variables are labeled as shown below

esdd: equivalent salt deposit density (mg/cm^2)

ld: leakage distance (cm)

fov: flashover voltage

lnesdd: natural log of esdd

lnld: natural log of leakage distance

lnfov: natural log of flashover voltage

The regression equation is

$$\text{lnfov} = -0.853 - 0.363\text{lnesdd} + 0.78\text{lnld} \qquad 5.1$$

The above equation can also be written as shown below

$$\text{fov} = .426 * \text{esdd}^{-0.363} * \text{ld}^{0.78} \qquad 5.2$$

The following table obtained from Minitab 16, shows the T-test statistic values and P values for the predictor variables

Predictor	**Coef**	**SE Coef**	**T**	**P**
Constant	-0.8529	0.1794	-4.76	0
lnesdd	-0.36335	0.02789	-13.03	0
lnld	0.78041	0.03742	20.86	0

S = 0.0712403 R-Sq = 97.6% R-Sq(adj) = 97.3%

PRESS = 0.114682 R-Sq(pred) = 96.36%

Analysis of Variance

Source	DF	SS	MS	F	P
Regression	2	3.0708	1.5354	302.53	0
Residual Error	15	0.0761	0.0051		
Total	17	3.1469			

Source	DF	Seq SS
Lnesdd	1	0.8632
Lnld	1	2.2076

Where,

SE Coef – Standard error coefficient

T – Standard “T” statistic

P – Probability of testing the significance of null hypothesis

F – Standard “F” statistic

S – Standard deviation

PRESS – Prediction error sum of squares

R-Sq – Residual sum of squares

R-Sq(adj) – Adjusted residual sum of squares

R-Sq(pred) – Predicted residual sum of squares

DF – Degrees of freedom

SS – Sum of squares

MS – Mean sum of squares

- The R^2 (adjusted) value for the above model is 97.3 %. The high value of the co-efficient of determination (R^2 (adjusted)) indicates that the model is capable of explaining the variability in a wide range.
- The PRESS statistic is a measure of how well a regression model will perform in predicting new data. The PRESS statistic can be used to compute an R^2 prediction statistic. The high value of R^2 prediction statistic is capable of explaining about 96% of the variability in predicting new observations.
- A high F ratio and a very low P value indicate that the model is highly significant.

Residual plots

The graphical analysis of residuals is a very effective way to investigate the adequacy of the fit of a regression model. The normal probability plot, plot of residuals against the fitted values and the plot of residuals are examined to verify the underlying assumptions made in regression.

Normal probability plot

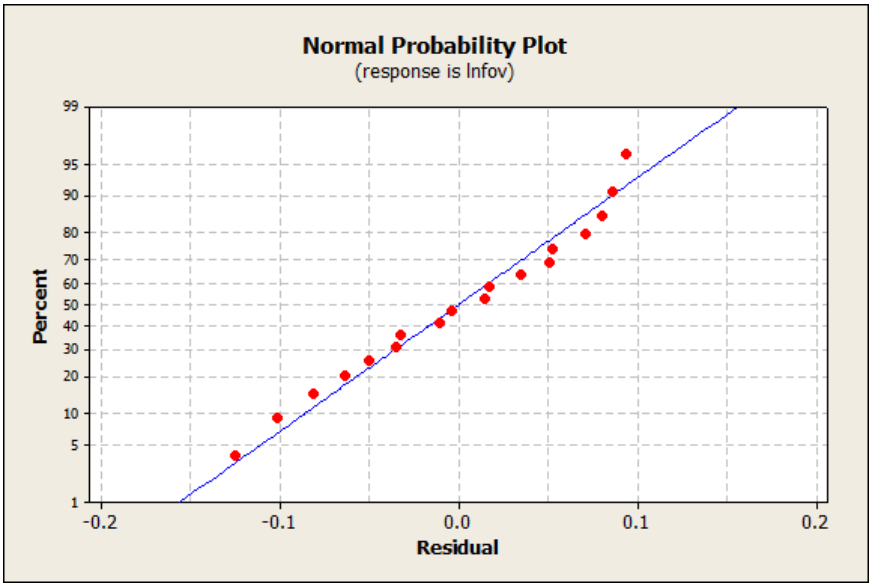

Figure 5.2 Normal probability plot for residuals

The above normal plot displays the points lying approximately on a straight line and therefore the error distribution is normal. The right tail of the plot bends slightly up. However, the plot is not grossly non-normal. Therefore regression analysis is robust to normality assumption.

Residuals versus fits

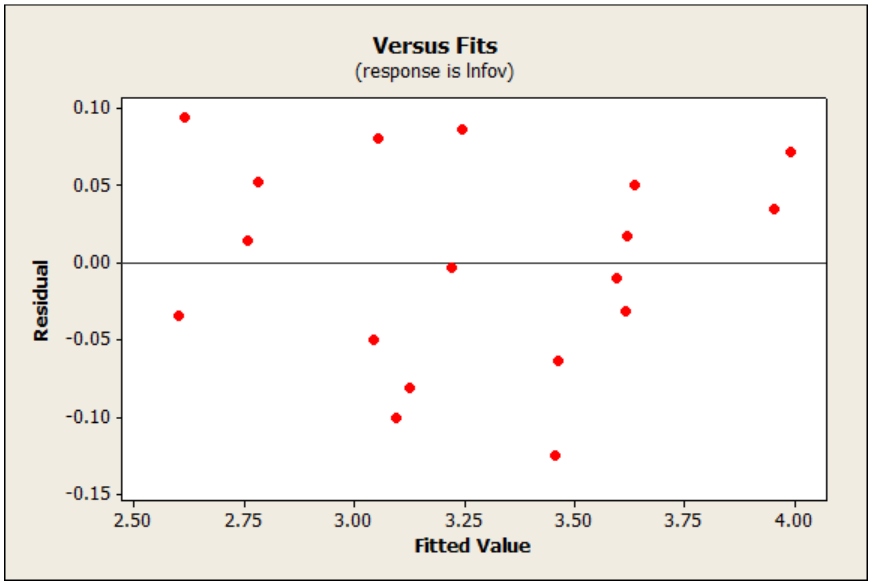

Figure 5.3 Residual v/s fitted values plot

The above plot indicates that the residuals can be contained in a horizontal band. The plot also does not depict any particular pattern which implies that there are no model defects.

RTV Silicone Rubber coated insulators

The wettability of the coated insulator was raised by washing the surface with water and isopropanol. The hydrophobicity classification of HC-4 to HC-5 was obtained and then the flashover experiments were carried out in the fog chamber. The following tables show the values obtained from the flashover tests performed on RTV silicone rubber coated insulators.

Voltage Class: 23 kV

Table 5.5 Flashover voltages for 23 kV voltage class at different levels of ESDD

Sample	**ESDD (mg/cm^2)**	**Leakage distance (cm)**	**Flashover voltage (kV)**
N2	0.15	61	26
N2	0.14	61	27
N1	0.32	61	20
N1	0.3	61	22
N4	0.5	61	17
N4	0.49	61	19

Voltage Class: 46 kV

Table 5.6 Flashover voltages for 46 kV voltage class at different levels of ESDD

Sample	**ESDD (mg/cm^2)**	**Leakage distance (cm)**	**Flashover voltage (kV)**
N5	0.11	109	46
N5	0.103	109	48
N7	0.32	109	35
N7	0.3	109	39
N3	0.49	109	27

Voltage Class: 69 kV

Table 5.7 Flashover voltages for 69 kV voltage class at different levels of ESDD

Sample	ESDD (mg/cm^2)	Leakage distance (cm)	Flashover voltage (kV)
N1	0.1	183	73
N2	0.12	183	70
N4	0.32	183	55
N4	0.33	183	48
N2	0.3	183	60
N1	0.32	183	58
N1	0.51	183	52
N3	0.52	183	48
N3	0.5	183	46

The regression equation obtained from Minitab 16 is as follows:

$$\ln(\text{fov}) = -0.915 - 0.286\ln(\text{esdd}) + 0.881\ln(\text{ld}) \qquad 5.3$$

The above equation can be written as

$$\text{fov} = .4 * \text{esdd}^{-0.286} * \text{ld}^{0.881} \qquad 5.4$$

The regression output table is

Predictor	Coef	SE Coef	T	P	VIF
Constant	-0.9154	0.1532	-5.97	0	
lnesdd	-0.2858	0.02513	-11.37	0	1.002
lnld	0.88084	0.03104	28.37	0	1.002

S = 0.0648164 R- Sq = 98.2% R-Sq(adj) = 97.9%

PRESS = 0.0930583 R-Sq(pred) = 97.6%

Analysis of Variance

Source	DF	SS	MS	F	P
Regression	2	3.8099	1.905	453.44	0
Residual Error	17	0.0714	0.0042		
Total	19	3.8814			

Source	**DF**	**Seq SS**
lnesdd	1	0.4278
lnld	1	3.3822

- The R^2 (adjusted) value for the fit is 97.9%, which indicates that the model is capable of explaining a wide range of variability.
- A high value of R^2 prediction (97.6%) indicates that the model is capable of explaining 97.6% variability in predicting new observations.
- A high value of F statistic and a low value of p statistic indicate that the model is highly significant.

Residual plots

Normal probability plot:

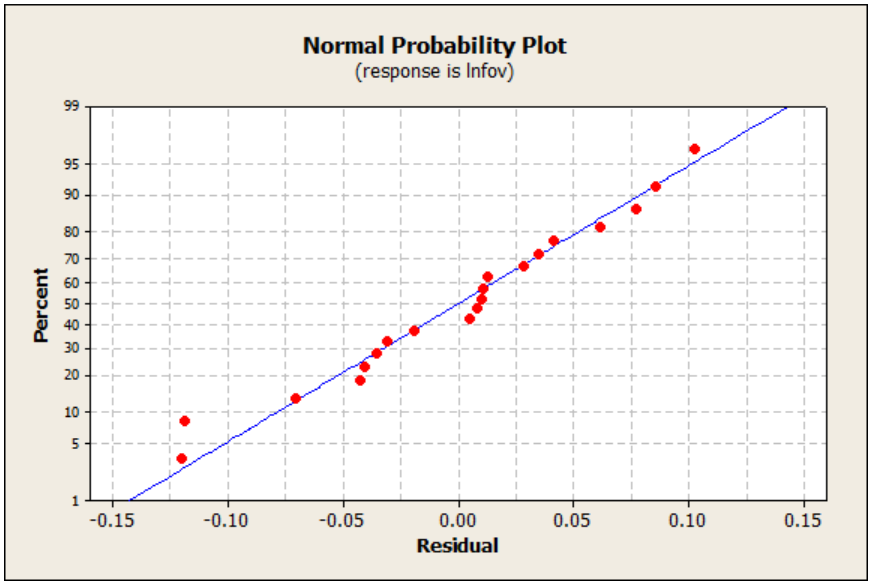

Figure 5.4 Normal probability plot for residuals

The above normal probability plot depicts the points lying approximately along a straight line. The error distribution is therefore normal.

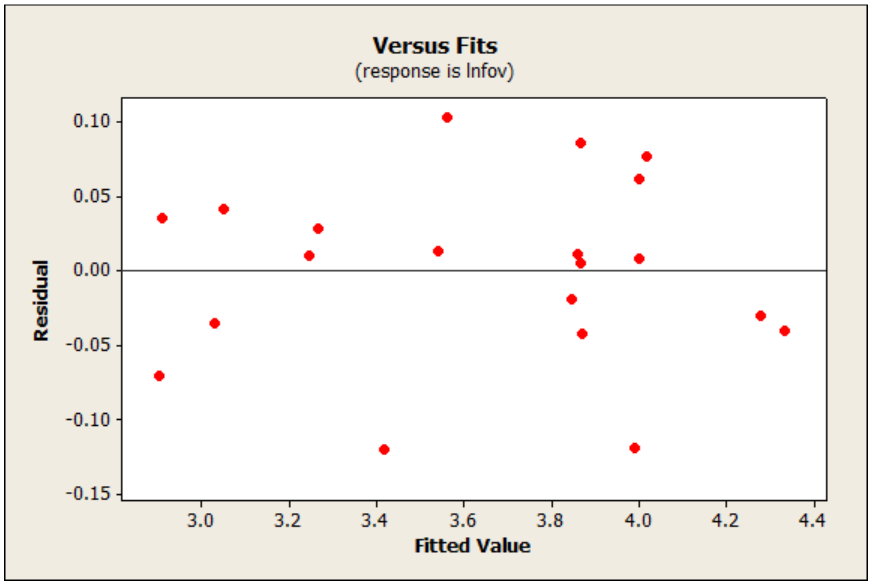

Figure 5.5 Residuals v/s fitted values plot

The residual versus fit plot shows that all the points lie in a horizontal band. There is no pattern and therefore the model is free from defects.

The equation 5.1 and 5.3 are plotted using Matlab shows the variation of flashover voltage with respect to different levels of contamination as well as leakage distance.

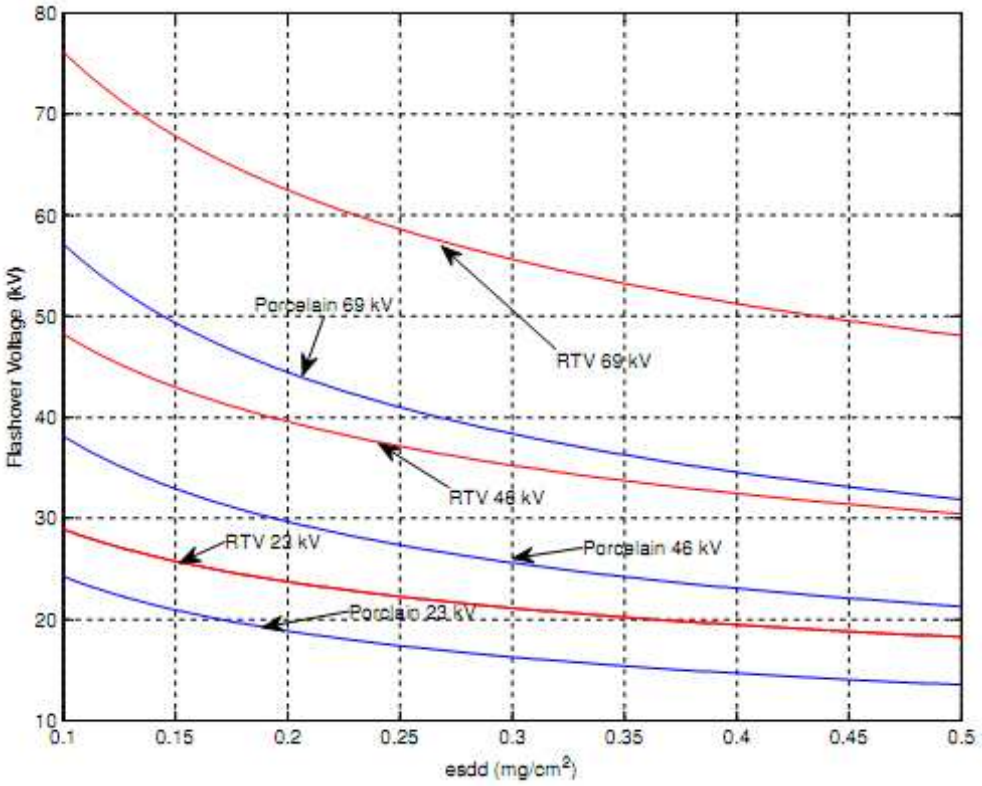

Figure 5.6 Flashover voltage v/s esdd (23-69 kV class)

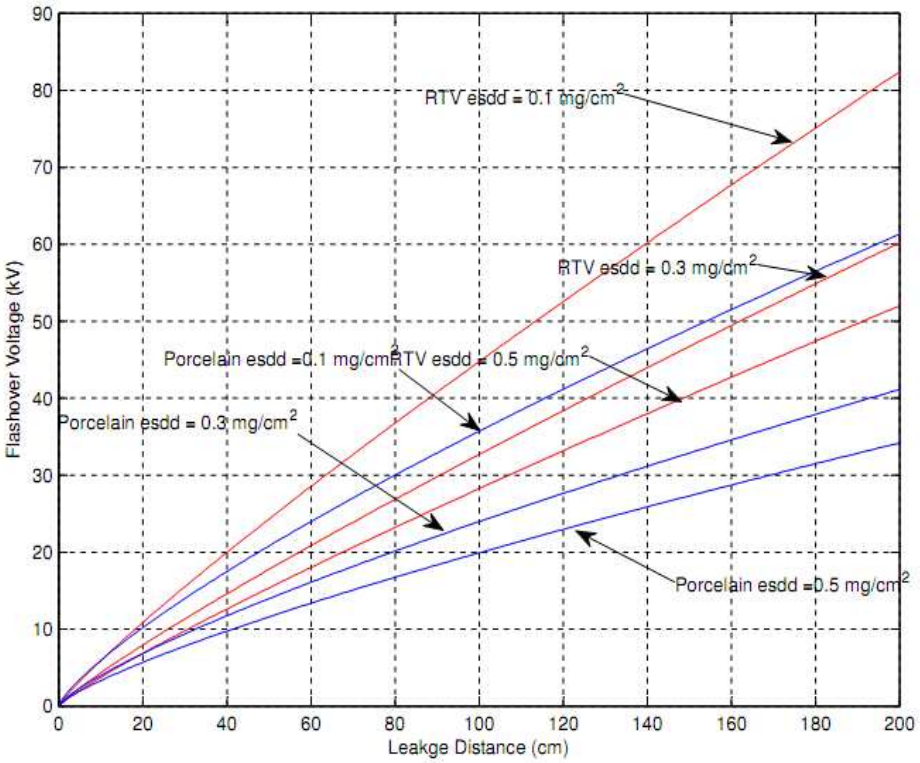

Figure 5.7 Flashover voltage versus leakage distance (23-69 kV)

5.3 Model validation

Comparison of the new model with earlier models

The model developed in this study is of the form

$$fov = A(ESDD^{-B})(ld^{C}) \qquad 5.5$$

Where,

fov: Flashover voltage in kV

A: Constant

ESDD: Equivalent Slat Deposit Density in mg/cm^2

B: Characteristic exponent for level of contamination

ld: Leakage distance in cm,

C: Characteristic exponent for leakage distance

For the new model developed in this study, the coefficients for the factors are as shown in the following tables

Table 5.8 Exponent comparison for the new model

Insulator type	**Constant A**	**Exponent B**	**Exponent C**
Porcelain	0.426	0.36	0.78
RTV SIR coated	0.4	0.28	0.88

Previous researchers have developed a regression model based on the severity of pollution i.e. ESDD and leakage distance. A model developed for porcelain post station insulators for HVDC applications by A.C. Baker, H. M. Schneider et al. incorporates only the severity of pollution. The model used the voltage corresponding to fifty percent probability of flashover denoted as critical flashover voltage (CFO).The effect of ESDD on flashover is expressed by the equation 5.6 [30].

$$CFO = A(ESDD^{-B}) \qquad 5.6$$

Where

CFO: Critical Flashover voltage in kV,

A: Constant,

ESDD: Equivalent salt deposit density in mg/cm^2

B: Characteristic exponent for level of contamination.

Similarly, a study on long rod SIR composite insulators was done by X. Jiang et al. and the model is as shown below [31].

$$U_f = A\left(SDD^{-B}\right) \quad 5.7$$

U_f: flashover voltage in kV,

A: Constant

SDD: Salt Deposit density in mg/cm^2,

B: Characteristic exponent.

The constant A in the equation depends on the profile of the insulators. B is the characteristic exponent characterizing the influence of the salt deposit density on the flashover voltages. The value of B depends on the conditions of partial arc burning, thus the environmental conditions, the test methods, the pollution materials and the material of the insulators will influence on it [31].

Table 5.9 Comparison for porcelain insulator model

Coefficient	**Baker & Schneider Model**	**New Model**
Constant A	18.34	0.426
Exponent B	0.32-0.41	0.36

For the Silicone Rubber coated insulators

Table 5.10 Comparison for polymer and RTV coated insulator model

Coefficient	**X.Jiang Model (SIR long rod)**	**New Model**
Constant A	126.34	0.4
Exponent B	0.24 - 0.3	0.28

- The exponent B value for the new model is however lower than that for the porcelain insulator.

- It is observed that the characteristic exponent B for the new model is the same range as the model developed by A.C .Baker, H.M. Schneider et al. However, in many cases the exponent B value (magnitude) in the Baker & Schneider model is greater than the exponent B value for the new model. This is because the DC flashover voltage is lower than the AC flashover voltage.
- The exponent B for RTV Coated Silicone Rubber and SIR long rod is in the same range for the new model and previous research works.
- The values of constant A in the new models are nearly the as the insulator samples had the same shed profile and geometry.
- The new model captures the effect of leakage distance on the flashover voltage effectively.

Energy loss calculation

Experiments were performed for studying the leakage current trends in porcelain and silicone rubber coated insulator. The test results of the leakage current pattern, cumulative leakage charges (Ampere-second calculation) and flashover voltages were compared to study the leakage current suppression performance in both the insulators. Porcelain and silicone rubber coated insulators were contaminated from medium to very high level for the experiment. It was ensured that the coated samples were hydrophilic. The test samples were subjected to voltages ranging from 2 – 20 kilovolts for 45 – 60 minutes inside the fog chamber.

Table 5.11 Data for the insulators used for leakage current tests

Insulator	**Surface material**	**ESDD (mg/cm^2)**	**Creepage path length (cm)**	**Specific creepage distance (mm/kV)**	**Number of sheds**
P	Porcelain	0.52	109	24	10
N4	RTV	0.51	109	24	10
P	Porcelain	0.11	109	24	10
N5	RTV	0.12	109	24	10

The leakage current monitoring system installed in the High Voltage Laboratory is capable of detecting peaks in each cycle for the 60 Hz sinusoidal waveform. The current signal sorts the peaks into data bins based on their magnitude. The peak leakage current is divided into the following levels:

Table 5.12 Current levels for the leakage current measurement test

Level 1	1-3 mA
Level 2	3-5 mA
Level 3	5-8 mA

The currents below 1 mA are neglected. Also it is important to note that the currents above 8 mA are not recorded due to limitations in the circuit.

Following are the results obtained from the tests:

ESDD: 0.5 mg/cm^2

The statistical summary of the cumulative peaks at different levels of applied voltage are as shown in the following bar graphs

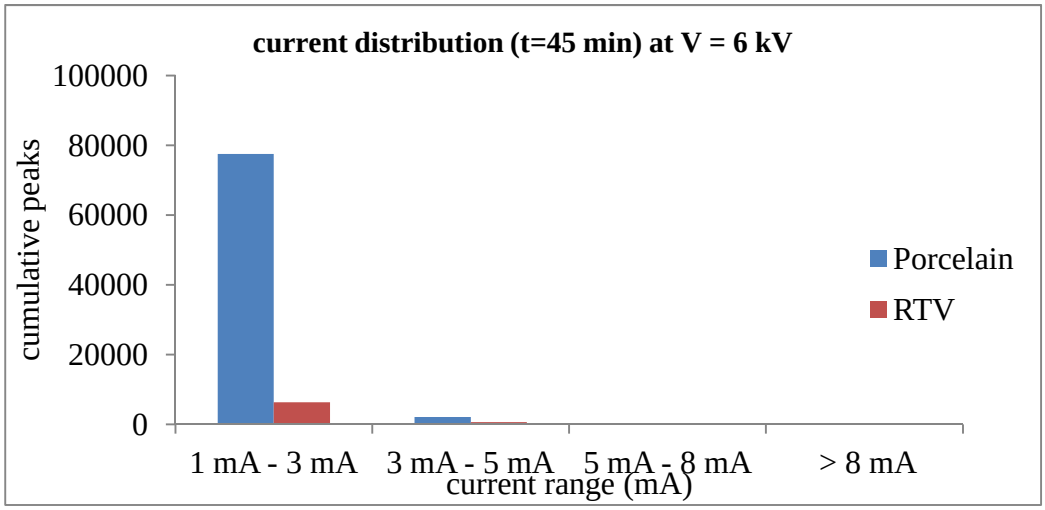

Figure 5.8 Bar graph diagram of recorded current peaks for porcelain insulator at V= 6 kV

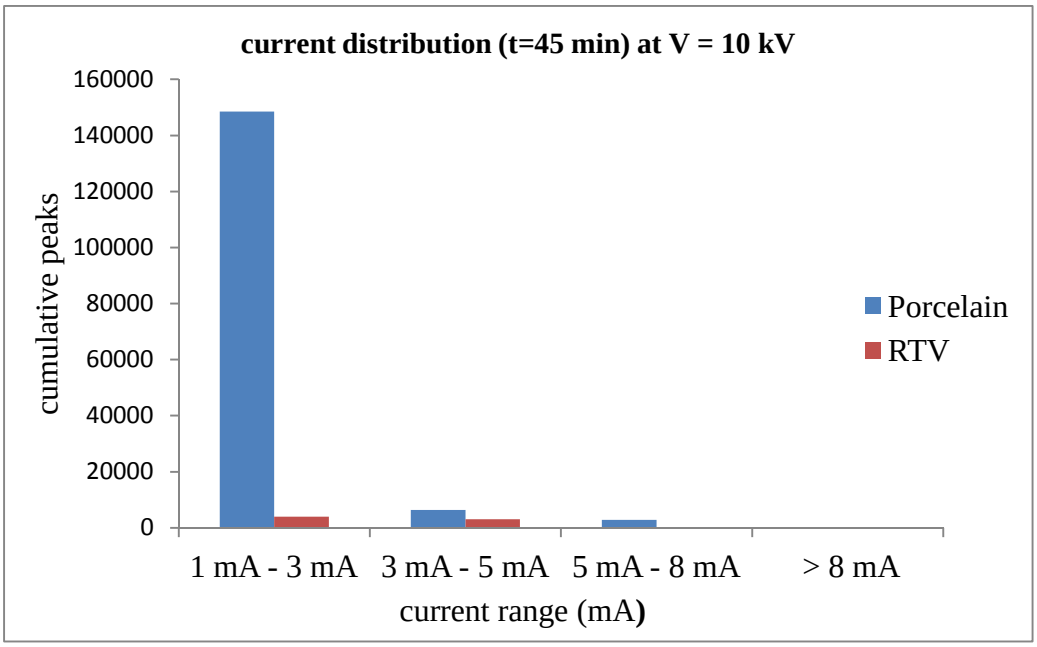

Figure 5.9 Bar graph diagram of recorded current peaks for porcelain insulator at V = 10 kV

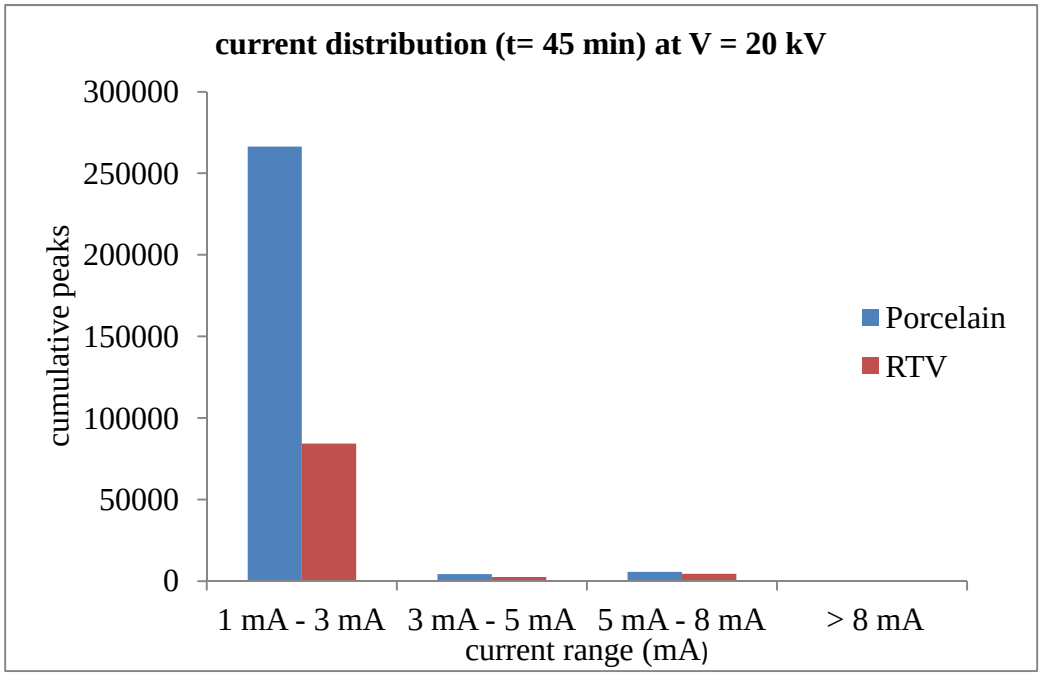

Figure 5.10 Bar graph diagram of recorded current peaks for porcelain insulator at V= 20 kV

From the above current distribution graphs it can be inferred that the leakage current on the RTV coated insulators is less than 1 mA for most of the time during the test. The leakage current on the porcelain insulator was higher than the hydrophilic RTV coated insulator.

For low voltages the cumulative peak distribution in 1-3 mA range is larger as compared to higher voltages. This is due to the increase in discharge activity at higher voltages which evaporates the moisture film on the insulator surface thereby decreasing the leakage current. It was observed that the discharge activity is significantly larger in the porcelain insulators than the silicone rubber coated insulators. The leakage current flow is choked due to sustained discharge activity on the surface of the RTV silicone rubber coated sample. Therefore the cumulative peaks for RTV coated are always less than that of porcelain throughout the entire current range.

The energy loss is calculated using the cumulative leakage charge build-up over the entire run of the experiment. The 60 Hz sinusoidal leakage current peaks are converted to equivalent RMS values and readings were noted for every five minute interval in the 45 minute run. The energy loss calculation incorporates the heat loss due to the flow of leakage current as well as dry band arcing.

Following graphs show the average RMS current readings for the experiments on porcelain and RTV coated insulators.

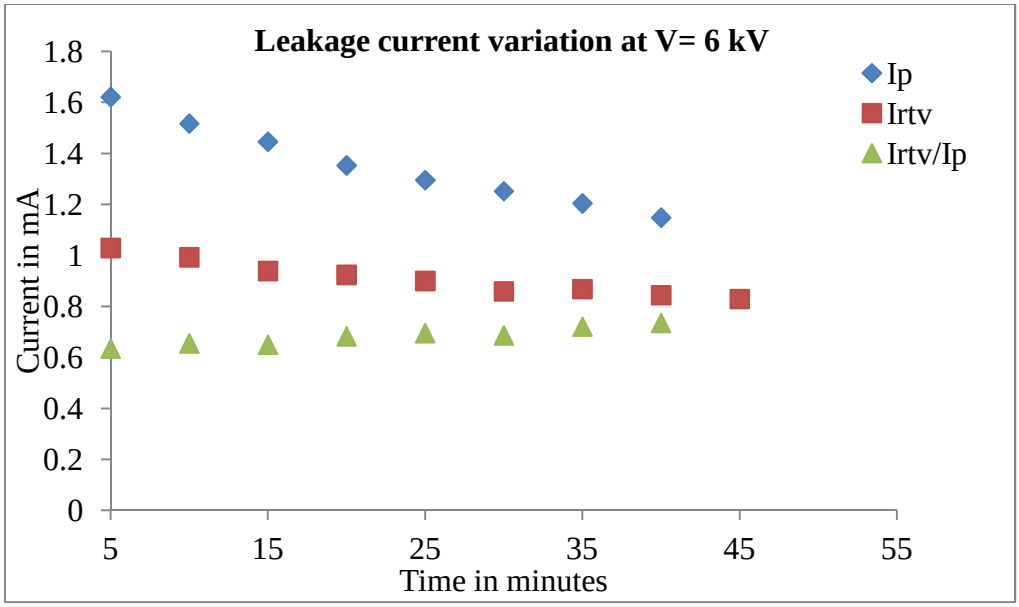

Figure 5.11 Typical variation of the leakage current for a 45 minute interval at V = 6 kV

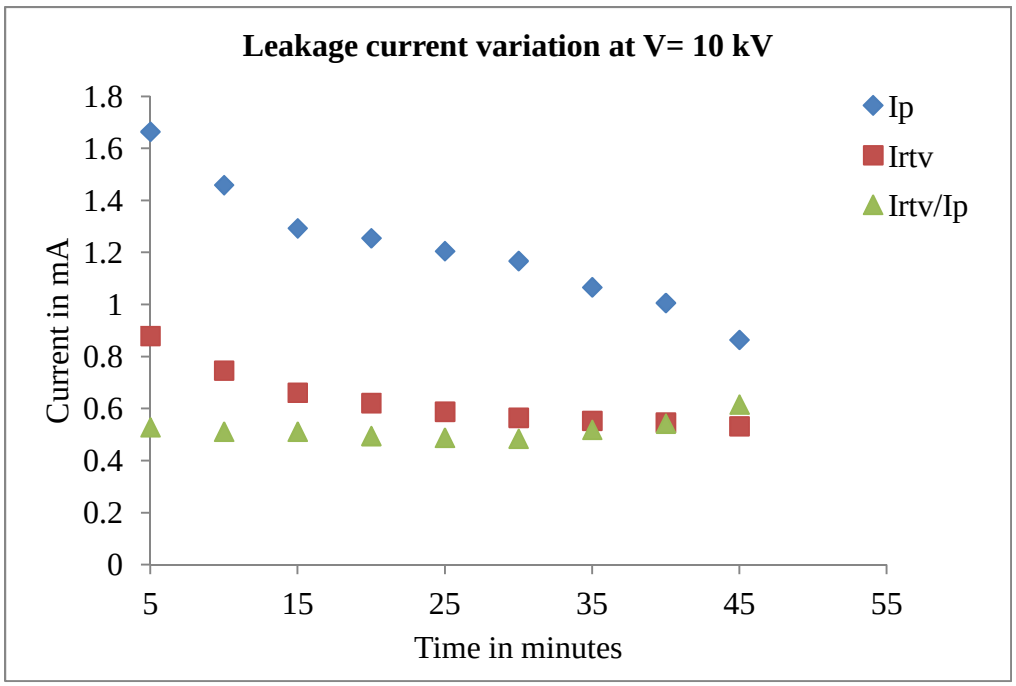

Figure 5.12 Typical variation of the leakage current for a 45 minute interval at V = 10 kV

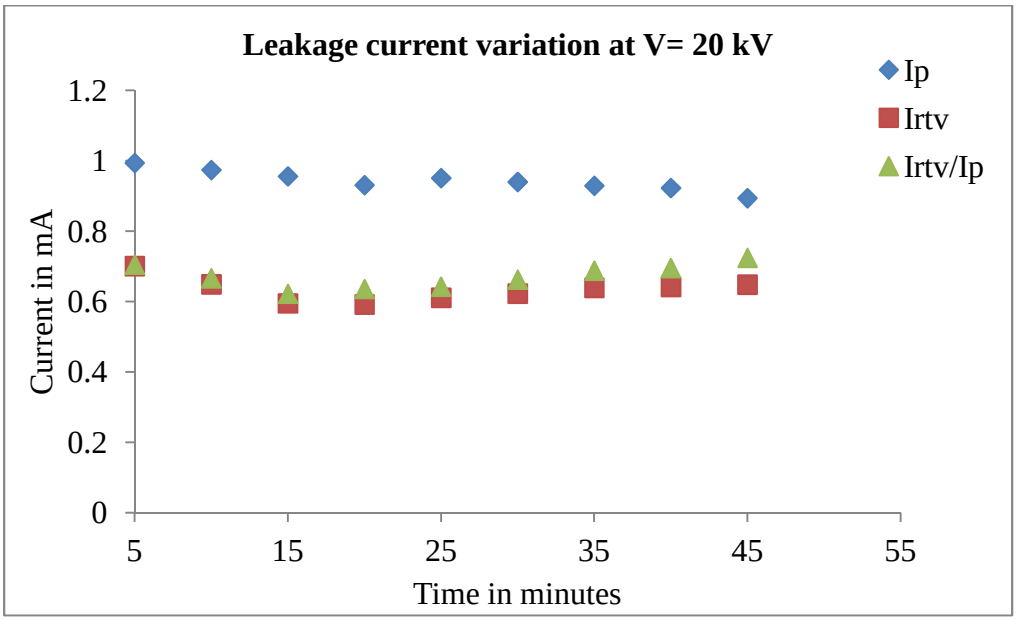

Figure 5.13 Typical variation of the leakage current for a 45 minute interval at V = 20 kV

The integration of leakage current with respect to time gives the leakage charge quantity. The applied voltage is constant throughout the experiment run. Therefore the energy loss can be calculated using the equation

$$E = \left[\int_{t_1}^{t_2} V.i(t).dt\right]/3600 \qquad 5.8$$

Where,

E: Energy dissipated during the entire test in Watt-hour

V: Voltage applied across the insulator in kV

i(t): Time varying leakage current flowing on the insulator surface in mA

t_1, t_2: time in minutes.

The following table shows the energy loss calculated for porcelain insulator and RTV coated insulators

Table 5.13 Energy loss calculation for porcelain insulator

V (kV)	E_P (W-hr)	E_{RTV} (W-hr)	Ratio
6	5.3	3.5	0.66
10	7.6	4.5	0.59
20	12.6	8.4	0.66

From the above table it can be inferred that the energy loss in the RTV coated insulators is about 59-66 % to that of porcelain insulators. This advantage is attributed to the suppression of leakage current on the RTV coated insulator. Contamination and wetting conditions govern the flow of leakage current on the insulator surface. Even when the hydrophobicity of the RTV coated insulator is lost temporarily, it does not permit complete wetting of the surface and therefore the flow of leakage current is less as compared to a completely hydrophilic porcelain surface. The surface resistance measured at 6

kV for the porcelain sample is 44 kΩ/cm and is 61 kΩ/cm for the RTV coated sample. At higher voltages, the heat due to high local current density evaporates the moisture and the surface begins to dry up. As a result the insulator surface with becomes coated with irregular water patches. At 10 kV, the surface resistance measured for the porcelain and RTV coated sample is 95 kΩ/cm and 160 kΩ/cm respectively. It is observed that the wetting action is more prominent on the porcelain surface. The improvement in flashover performance is around 28% - 35% for a severely contaminated case.

ESDD: 0.1 mg/cm^2

Similar experiments were carried out for a medium level of pollution severity. The leakage current statistics for different voltage levels are as shown below.

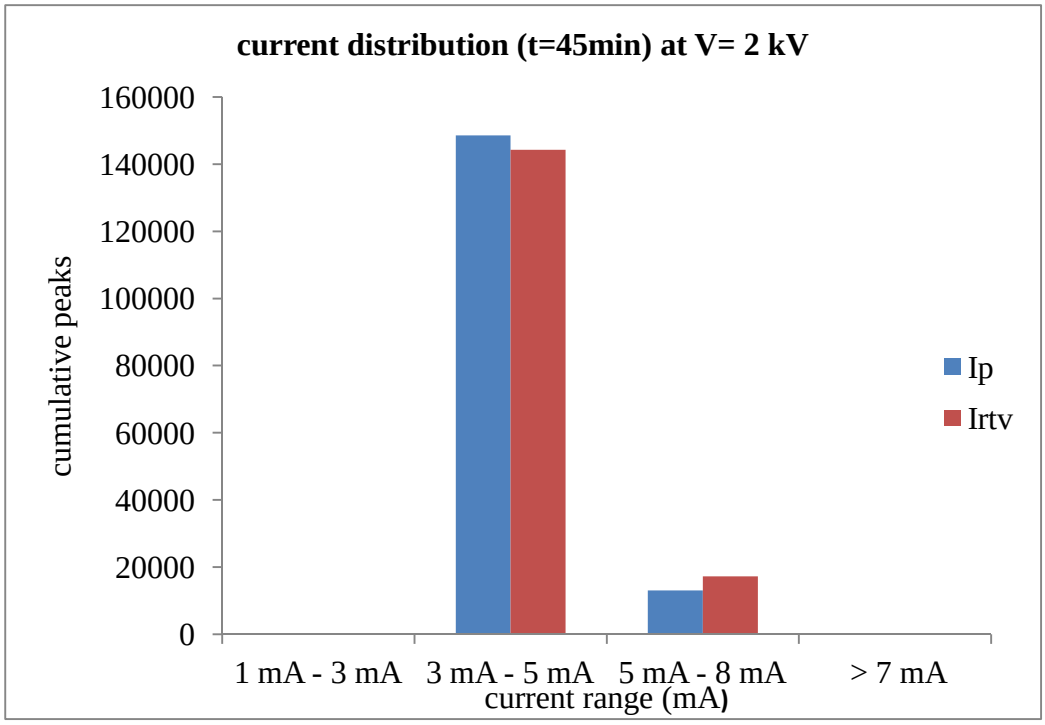

Figure 5.14 Bar graph diagram of recorded current peaks for porcelain insulator at V= 2 kV

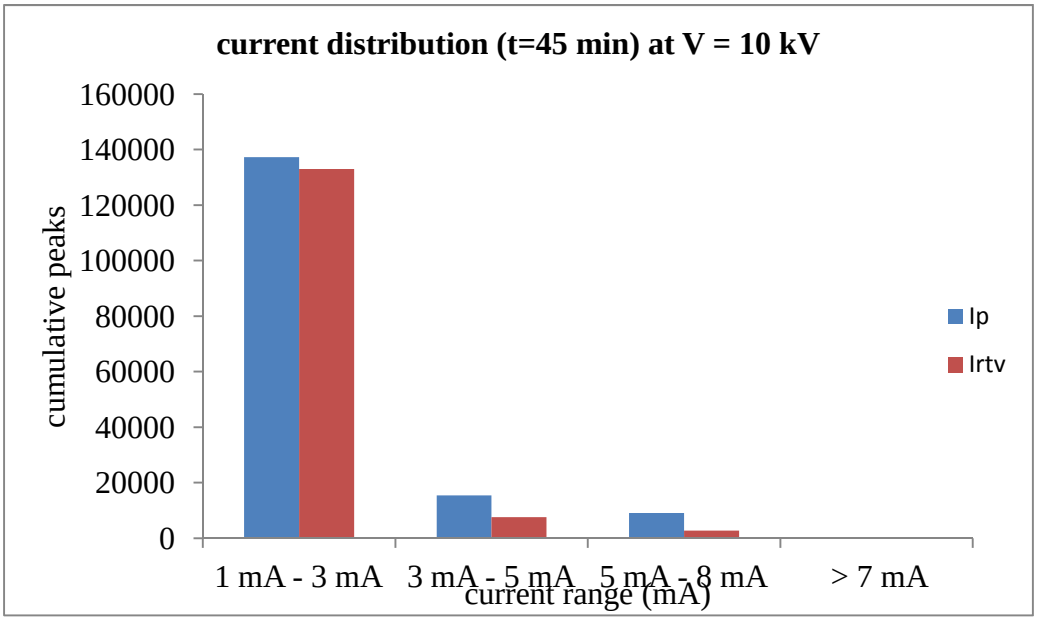

Figure 5.15 Bar graph diagram of recorded current peaks for porcelain insulator at V= 10 kV

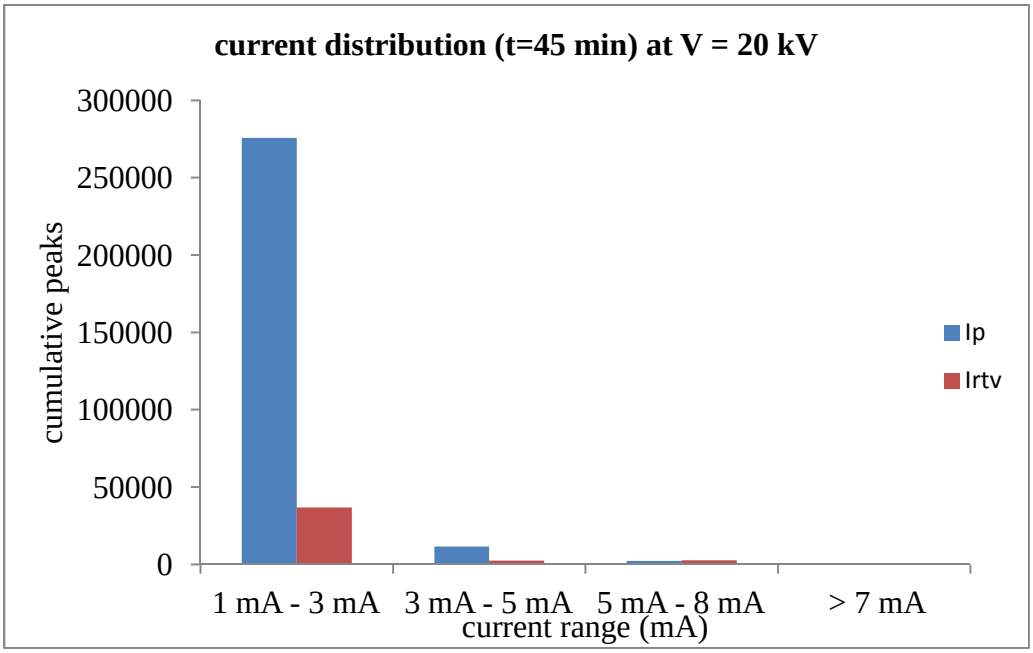

Figure 5.16 Bar graph diagram of recorded current peaks for porcelain insulator at V= 20 kV

From the figure, it is seen that the leakage current on the porcelain and silicone rubber coated insulators is nearly the same at 2 kV. The current leakage current lies in the

1-3 mA range for most of the time in the experiment. Also the current distribution for both the samples is similar at 10 kV. However, the ratio of leakage current on silicone rubber coated insulators to the current on the porcelain insulator is less than 1 always. The nearly equal leakage currents on both the insulator samples can be explained by the superior self-cleaning property of the glazed porcelain surfaces than from the silicone rubber surfaces [32]. The surface resistance measured at 2 kV for porcelain and RTV coated insulator is 6 kΩ/cm and 7.6 kΩ/cm respectively. However, there is a significant difference between the surface resistances for the samples measured at 10 kV. The surface resistance for RTV coated insulator is 110 kΩ/cm, while for the porcelain insulator it is 77 kΩ/cm. At a higher voltage i.e. at 20 kV, a significant discharge activity was observed on both the samples. The surface resistance measured at 20 kV is higher as the dry band arcing evaporates the water accumulated on the surface, thereby reducing the leakage current. The surface resistances measured at 20 kV are 230 kΩ/cm and 325 kΩ/cm for porcelain and RTV coated insulators respectively.

The following graphs show the leakage current variation for the porcelain and RTV coated samples at medium severity.

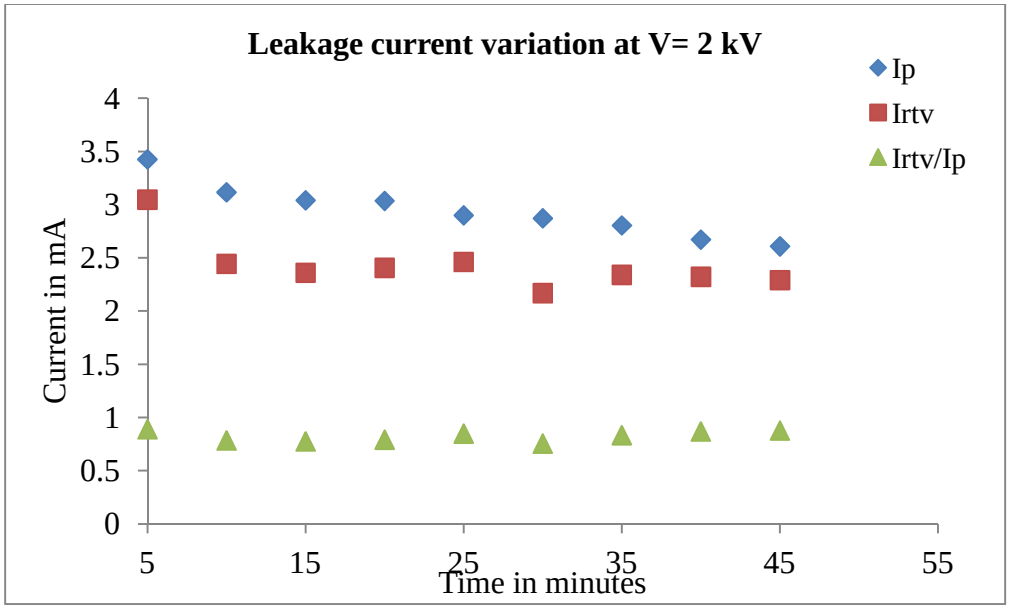

Figure 5.17 Typical variation of the leakage current for a 45 minute interval at V = 2 kV

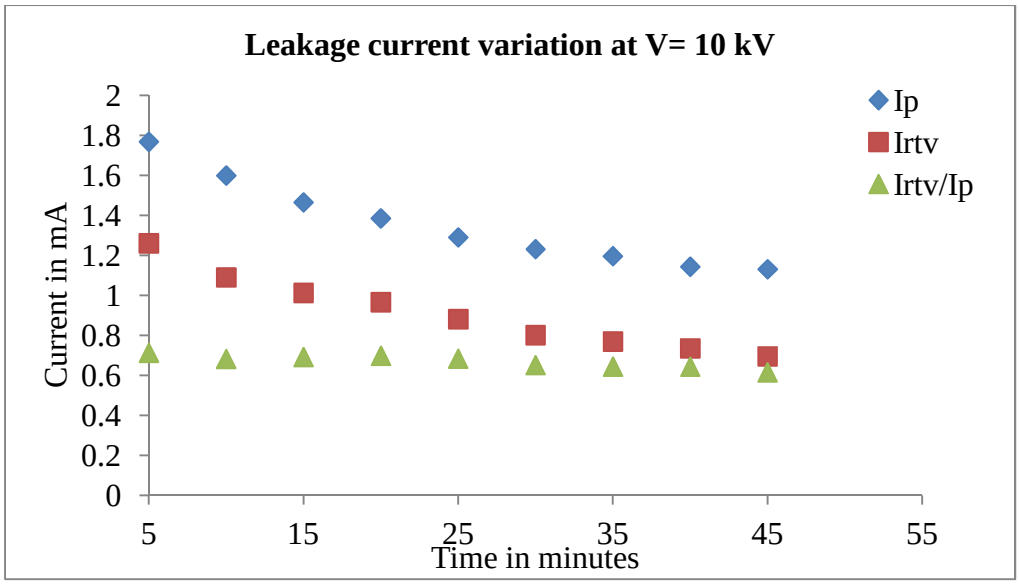

Figure 5.18 Typical variation of the leakage current for a 45 minute interval at V = 10 kV

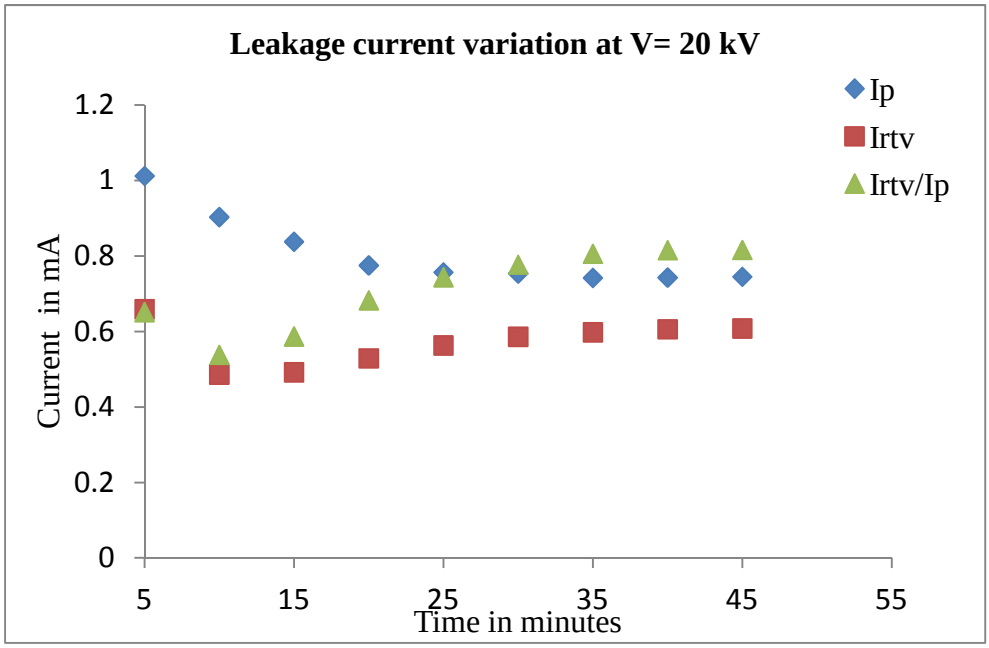

Figure 5.19 Typical variation of the leakage current for a 45 minute interval at V = 20 kV

The table below shows the energy loss calculation in the porcelain and RTV coated insulators.

Table 5.14 Energy loss calculation for RTV silicone rubber coated insulator

V (kV)	E_P (W-hr)	E_{RTV} (W-hr)	Ratio
2	4	3.2	0.8
10	8.9	6	0.67
20	10.7	7.6	0.71

The energy dissipation on the RTV coated insulator surface is from 67-80 % to that in porcelain insulators. The improvement in flashover at medium pollution severity is 20% as seen from the flashover tests.

5.4 FTIR Analysis

The RTV silicone rubber is popularly used in station insulators because of their ability to provide a high surface resistance in presence of contamination and moisture. The high surface resistance is due to the non-wettability of the coatings. The hydrocarbons, fluorocarbons and silicones generally have low surface energy [33]. The RTV silicone rubber coating is made from a basic polydimethylsiloxane (PDMS) polymer which is a basic molecule for silicone oil and silicone rubber. The molecular structure for PDMS is as shown below [33, 34].

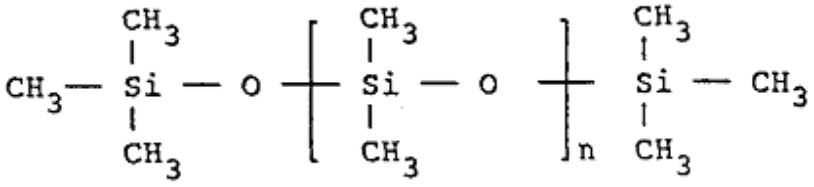

Figure 5.20 Chemical structure of PDMS molecule

The wettability of the coating is due to the methyl groups in the silicone. Previous research work has suggested that the hydrophobic silicone coating can be changed to one that is hydrophilic due to a reorientation of surface molecules with moisture, such as fog or rain. It is also suggested that the dry band arcing also bring the physical and chemical changes.

Fourier Transform Infrared Spectroscopy (FTIR) analysis was carried out on the coating samples. The samples compared in this study were:

Sample 1	Virgin RTV Silicone Rubber
Sample 2	Hydrophilic sample N3 (HC-5)
Sample 3	Hydrophobic sample N4 (HC-2)

A Thermo Nicolet 6000 FTIR instrument was used with Smart Orbit % Transmittance accessory for performing the analysis on the samples. Special care was taken that the crystal in the instrument was cleaned using methanol after each IR test. The FTIR plot for a virgin RTV coating is as shown below.

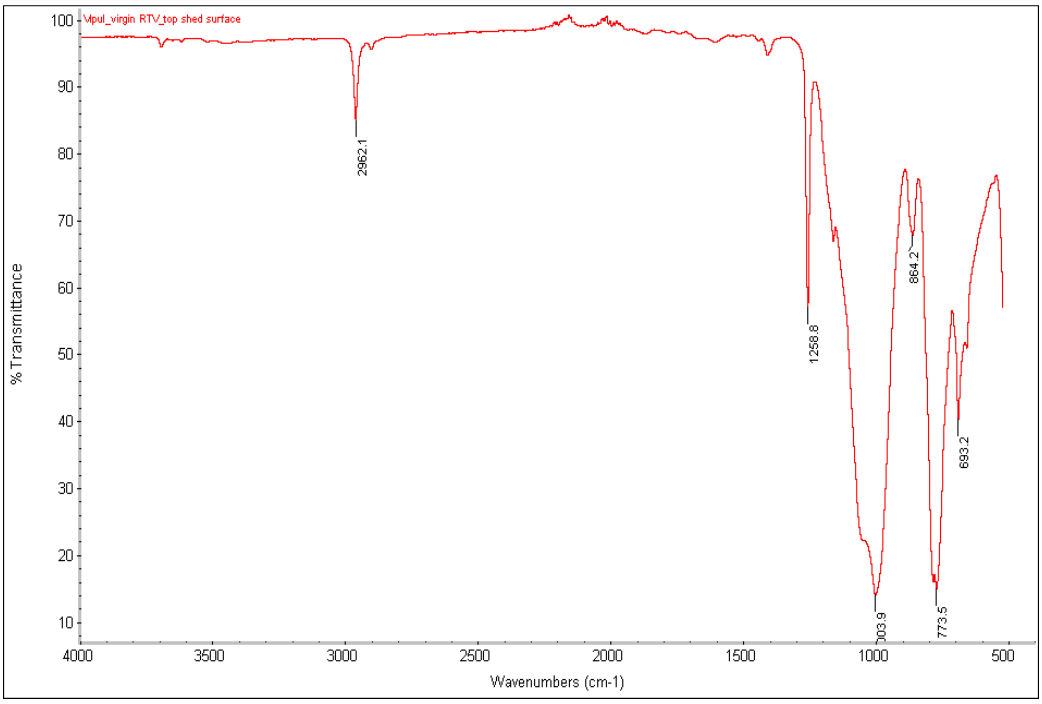

Figure 5.21 FTIR plot for virgin RTV coating (top shed surface)

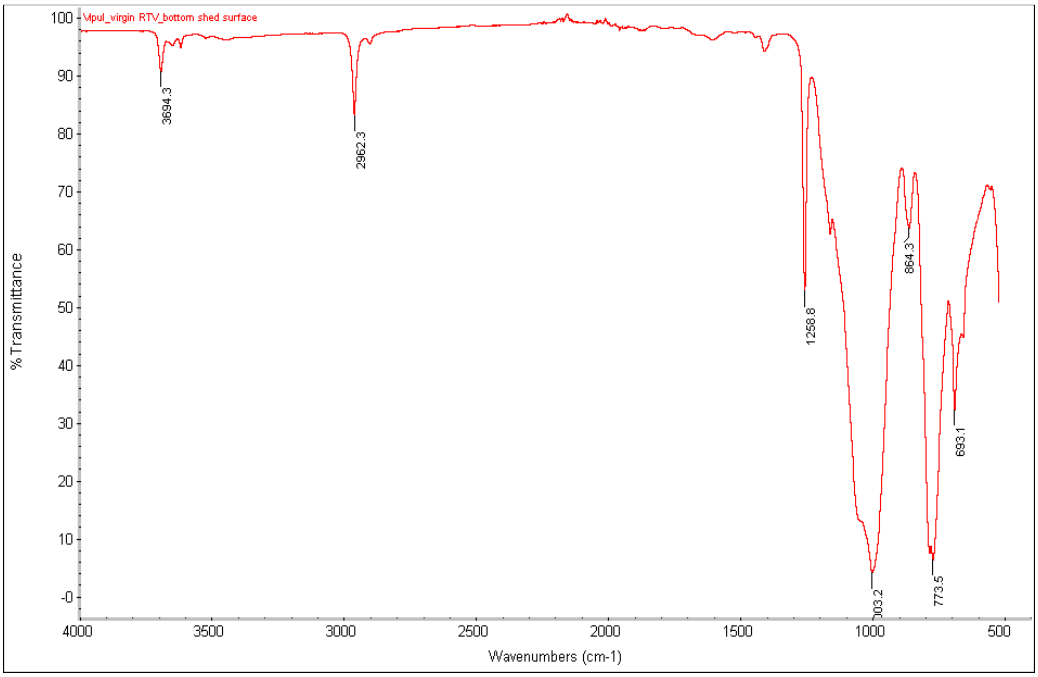

Figure 5.22 FTIR plot for virgin RTV (bottom shed surface)

The typical IR absorption bands observed in the silicone rubber samples are as shown in the table below [34]

Table 5.15 IR Absorption Bands

Absorption Band Number	**Wave Number (cm^{-1})**	**Bond**
1	3700-3200	OH
2	2962-2910	CH in CH_3
3	1270-1255	Si-CH_3
4	1100-980	Si-O-Si
5	980-850	Si-$(CH_3)_3$
6	840-790	Si-$(CH_3)_2$
7	750-640	Si-$(CH_3)_3$

The following figure shows the FTIR plots obtained for the top surface of the silicone rubber coated shed for samples N3 and N4.

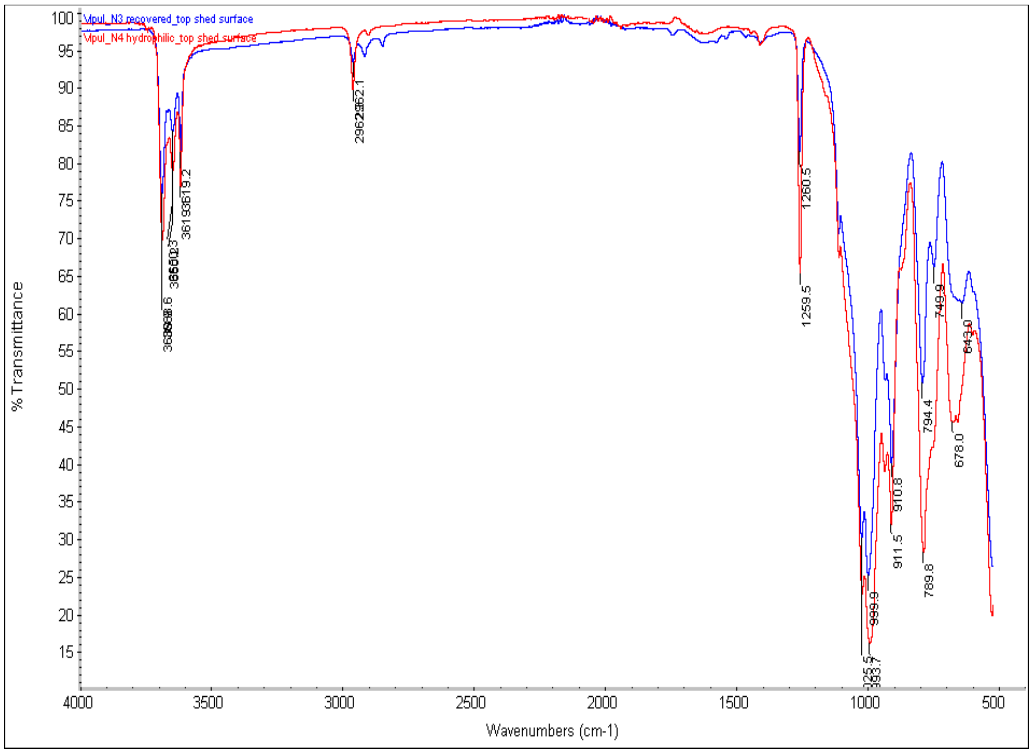

Figure 5.23 Sample N3 v/s Sample N4 (top shed surface)

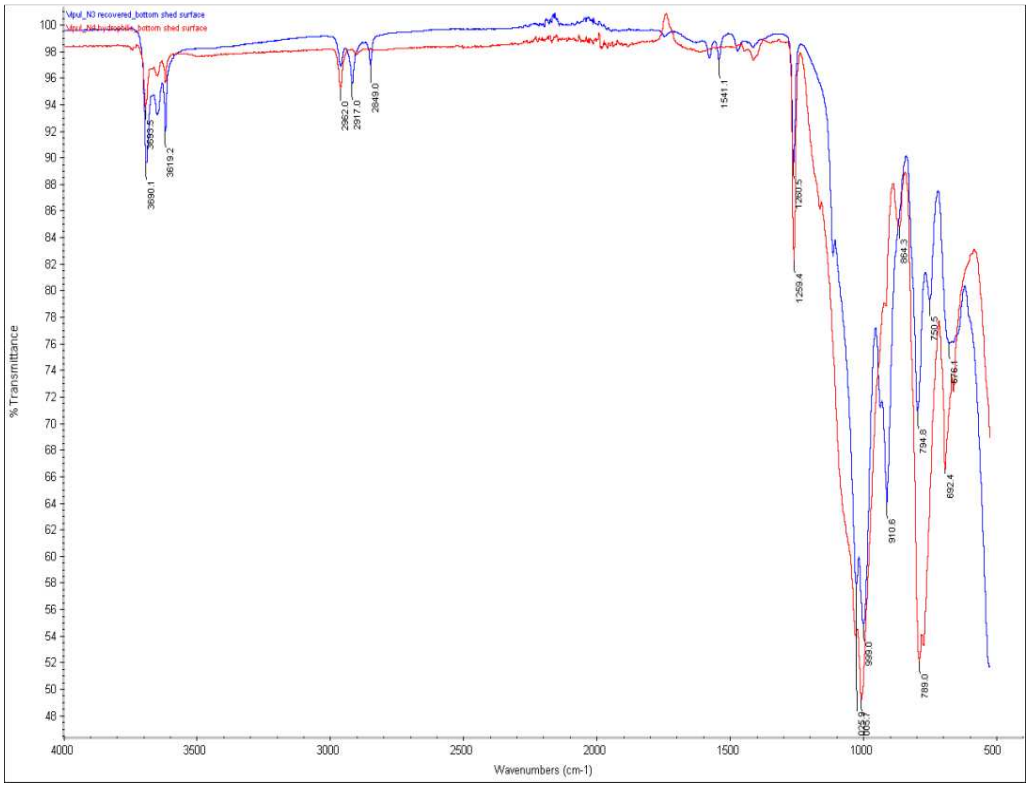

Figure 5.24 Sample N3 v/s Sample N4 (bottom shed surface)

Sample N3 and N4 were both subjects to high voltage tests. While performing the FTIR test the sample N3 was allowed to recover. After a rest time of 4 days the sample N3 was hydrophobic.

From the above figure the following observations are made:

- The peak at 3450 cm^{-1} was not detected in any of the samples, which indicates that there is no Alumina Trihydrate (ATH) filler [35].
- The IR absorption intensity in band 3 (1270-1250 cm^{-1}) decreased. This can be verified by the increase in the % transmittance from the plot. Similar observation was noted in band 2 (2962-2910 cm^{-1}). The decreased absorption is due to CH deformation in Si-CH_3 group i.e. decreased CH_3 groups at the surface [33, 34].

- The absorption intensity in group 7 (750-640 cm^{-1}) for the recovered sample N3 decreased as compared to the hydrophilic and virgin silicone rubber samples. The dry band arcing during the tests removed some CH3 groups from the side chains of PDMS deforming the molecule.
- For the hydrophobic sample N3, the absorption intensity in band 6 is higher than the intensity in band 7.
- The absorption intensity in band 4 (1100-980 cm^{-1}) has increased, which indicates that the molecular structure of the polymer has changed. The absorption in this band is from the Si-O-Si bond (cyclic trimers of PDMS). Previous research works indicates that the cyclic trimers combining with each other, give molecules that are cross linked randomly in three dimensions [33].
- The samples subjected to high voltage tests showed absorption in 3750-3200 cm^{-1} region indicating the OH stretching vibration of the Si-OH groups [34]. No such signs were observed in the virgin RTV sample.
- Similar observations are made for the coating at the bottom shed surface for N3 and N4. It was noticed that the absorption is more in the bottom shed coating than the top surface coating for every band.

Chapter 6. Conclusions and Future Work

6.1 Conclusions

The study was aimed at providing a quantitative performance comparison between uncoated and RTV silicone rubber coated station post insulators. The main conclusions from the study are as follows

- A statistical model based on regression analysis, that predicts the flashover voltages of RTV silicone rubber and bare porcelain station post insulators under the influence of coastal contamination is developed. The model was validated using clean fog tests and model data from other independent researchers. The following models were developed for the coated and uncoated samples from the experimental findings.

$$\text{Porcelain insulators: } Fov = .42esdd^{-0.36}ld^{0.78}$$

$$\text{RTV silicone rubber insulators: } Fov = .4esdd^{-0.28}ld^{0.88}$$

- RTV coated posts withstood much higher levels of contamination (measured in esdd) when compared to bare porcelain. This was the case when the coating has completely lost its hydrophobicity. The hydrophobicity loss was created by spraying isopropyl alcohol on the coated insulators. At medium esdd level (0.1 mg/cm2) the coating on posts provides an improvement of 20 % in the flashover performance when it is hydrophilic. However, at high contamination severity (esdd level 0.5 mg/cm2) an improvement up to 35 % in flashover performance was observed as compared to the uncoated posts. The disparity in the results at low contamination level is due to the superior self-cleaning property of the porce-

lain surface which reduces the actual amount of pollution accumulated on the surface.

- The adhesion of the RTV silicone rubber coatings to the porcelain was excellent. This was even after many tests where there was a significant discharge activity during the tests.
- RTV coated porcelain posts can for a reduced height give same or better performance than taller posts or posts with extended leakage distance.

6.2 Future work

- The model developed in this study predicts the failure of station post insulators used at a sub-transmission voltage level i.e. from 25 kV – 69 kV. The approach can be used to develop models for flashover prediction at high voltage levels. The fog withstand voltage – leakage distance characteristics shows a tendency of non-linearity at higher leakage distances. This behavior needs to be appropriately modeled for a better prediction of flashover at higher voltages.
- The insulator samples used in the study had the same shed configuration. For a general model insulators with different geometries or shed configuration need to be considered.
- The model for silicone rubber coated insulators does not incorporate the degradation of the coating. A new model that accounts for ageing of the surface in addition to the parameters used in the current model can be looked into the future for coated insulators

REFERENCES

[1] S. Venkataraman, “Prediction of flashover voltage for outdoor insulators,” Ph. D. Disssertation, Arizona State University, December 2007

[2] EPRI, “Transmission line reference book – 345 kV and above,” Second Edition 1987.

[3] Wang Daxing, Xu An, Liu Ping, Cui Tao, “Flashover mechanism and prevention measures of polluted insulators in power system,” Power and Energy Engineering Conference (APPEEC), 2011 Asia-Pacific, Vol., No., pp.1-4, 25-28 March 2011.

[4] Group, I.W., “A survey of the problem of insulator contamination in the United States and Canada-Part I,” IEEE Transactions on Power Apparatus and Systems, Vol.PAS-90, No.6, pp.2577-2585, Nov. 1971.

[5] The Authoritative Dictionary of IEEE Standards Terms, IEEE Std 100, 2000.

[6] Notes on, “Composite insulator age overview,” Available at http://www.polymer-insulators.com/list1.asp?id=296, September 2012.

[7] N. Vasudev, “Design of external insulation from the point of view of pollution: 2010,” Available: http://conf05.iitkgp.ac.in/icps09/photoppt/ppt/nv.pdf

[8] E. A. Cherney, “RTV silicone-a high tech solution for a dirty insulator problem,” Electrical Insulation Magazine, IEEE, Vol.11, No.6, pp.8-14, Nov.-Dec. 1995.

[9] W. McDermid, T. Black, “Experience with Preventing External Flashovers in HVDC Converter Stations,” Conference Record of the 2008 IEEE International Symposium on Electrical Insulation, Vol., No., pp.81-84, 9-12 June 2008.

[10] S. M. Gubanski, A. E. Vlastos, “Wettability of naturally aged silicon and EPDM composite insulators,” IEEE Transactions on Power Delivery, Vol.5, No.3, pp.1527-1535, Jul 1990.

[11] E. A. Cherney, R. Hackam, S. H. Kim, “Porcelain insulator maintenance with RTV silicone rubber coatings,” IEEE Transactions on Power Delivery, Vol.6, No.3, pp.1177-1181, Jul 1991.

[12] M. Farzaneh, W. Chisholm, “Insulators for icing and polluted environments,” John Wiley and Sons, Inc., Publication

[13] R. E. Carberry, H. M. Schneider, “Evaluation of RTV coating for station insulators subjected to coastal contamination,” IEEE Transactions on Power Delivery, Vol.4, No.1, pp.577-585, Jan 1989.

[14] IEC 815 Selection and Dimensioning of High Voltage Insulators for Polluted Conditions, Std., 1986.

[15] STRI Guide 92/1, Hydrophobicity Classification Guide, Swedish Technical Research Institute, 1992.

[16] E. Nasser, "Contamination flashover of outdoor insulation," Electroteknik + Automation, (ETZ-A), VDE-Verlag, Vol. 93, No. 6, pp. 321-325.

[17] A. J. Phillips, D. J. Childs, and H. M. Schneider, "Aging of non-ceramic insulators due to corona from water drops," IEEE Transactions on Power Delivery, Vol. 14, No. 3, pp. 1081-1089, July 1999.

[18] J. P. Holtzhausen, "A critical evaluation of AC pollution flashover models for HV insulators having hydrophilic surfaces," Ph.D. Dissertation, The University of Stellenbosch, 1997.

[19] R. Sundararajan, R.S. Gorur, "Dynamic arc modeling of pollution flashover of insulators under DC voltage," IEEE Transactions on Electrical Insulation, Vol.28, No.2, pp.209-218, Apr 1993.

[20] L. L. Alston, S. Zoledziowski, "Growth of discharges on polluted insulation," Proceedings of the Institution of Electrical Engineers, Vol.110, No.7, pp.1260-1266, July 1963.

[21] B. F. Hampton, "Flashover mechanism of polluted insulation," *Proceedings* of the Institution of Electrical Engineers, Vol.111, No.5, pp.985-990, May 1964.

[22] P. Claverie, Y. Porcheron, "How to choose insulators in polluted areas," IEEE Transactions on Power Apparatus and Systems, Vol.PAS-92, No.3, pp.1121-1131, May 1973.

[23] P. Claverie, "Predetermination of the Behaviour of Polluted Insulators," IEEE Transactions on Power Apparatus and Systems, Vol.PAS-90, No.4, pp.1902-1908, July 1971.

[24] R Sundarajan, "Dynamic arc modeling of pollution flashover of insulators energized with direct current voltage," Ph.D. Dissertation, Arizona State University, 1993.

[25] D. Montgomery, "Design and analysis of experiments," John Wiley and Sons, Inc., Seventh Edition, 2009.

[26] D. Montgomery, E. Peck, G. Vining, "Introduction to Linear Regression Analysis," John Wiley and Sons, Inc., Third Edition, 2003.

[27] Notes on, "Assumptions for Regression Analysis," available at: http://www.murraylax.org/m230/spring2009/assumptions_print.pdf

[28] IEEE Standard Techniques for High Voltage Testing, IEEE Std-4, 1995.

[29] G. Iyer, "Evaluation of electrical performance of medium voltage epoxy insulated equipment," M.S. Thesis, Arizona State University, August 2009.

[30] A. C. Baker, L. E. Zaffanella, L. D. Anzivino, H. M. Schneider, J. H. Moran, "Contamination performance of HVDC station post insulators," IEEE Transactions on Power Delivery, Vol.3, No.4, pp.1968-1975, Oct 1988.

[31] X. Jiang et al., "Study on pollution flashover performance of short samples of composite insulators intended for 800 kV UHV DC," IEEE Transactions on Dielectrics and Electrical Insulation, Vol. 14, No. 5, October 2007.

[32] K. L. Chrzan, W. L. Vosloo, J. P. Holtzhausen, "Leakage current on porcelain and silicone insulators under sea or light industrial pollution," IEEE Transactions on Power Delivery, Vol.26, No.3, pp.2051-2052, July 2011.

[33] S-H. Kim, E. A. Cherney, R. Hackam, "Suppression mechanism of leakage current on RTV coated porcelain and silicone rubber insulators," IEEE Transactions on Power Delivery, Vol.6, No.4, pp.1549-1556, Oct 1991.

[34] S-H. Kim; E. A. Cherney, R. Hackam, K. G. Rutherford, "Chemical changes at the surface of RTV silicone rubber coatings on insulators during dry-band arcing," IEEE Transactions on Dielectrics and Electrical Insulation, Vol.1, No.1, pp.106-123, Feb 1994.

[35] R. S. Gorur, J. Mishra, R. Tay, R. McAfee, "Electrical performance of RTV silicone rubber coatings," IEEE Transactions on Dielectrics and Electrical Insulation, V ol.3, No.2, pp.299-306, Apr 1996.

APPENDIX A

MATLAB CODE FOR FLASHOVER VOLTAGE PLOTS

A.1 Matlab code for flashover voltage plots

```
% Porcelain insulator model
clear all; clc
esdd = 0.1:0.001:0.5;ld=61; k=size(esdd); j=k(2);
for i=1:j
   LnFOV(i)=-0.853-0.363*log(esdd(i))+0.780*log(ld);
end
plot(esdd,exp(LnFOV),'b');
hold on;
grid on;

clear all;clc;
esdd = 0.1; ld=0:1:200; k=size(ld); j=k(2);
for i=1:j
   LnFOV(i)=-0.853-0.363*log(esdd)+0.780*log(ld(i));
end
plot(ld,exp(LnFOV),'b');
hold on;
grid on;

% RTV Silicone Rubber coated insulator model
clear all;clc;
esdd = 0.1:0.001:0.5; ld=61; k=size(esdd); j=k(2);
for i=1:j
   LnFOV(i)=-0.915-0.286*log(esdd(i))+0.881*log(ld);
end
plot(esdd,exp(LnFOV),'r');
hold on;
grid on;

clear all; clc;
esdd = 0.1;ld=0:1:200;k=size(ld);j=k(2);
for i=1:j
   LnFOV(i)=-0.915-0.286*log(esdd)+0.881*log(ld(i));
end
plot(ld,exp(LnFOV),'r');hold on; grid on;
```

APPENDIX B

SURFACE RESISTANCE MEASUREMENTS

B.1 Surface resistance measurements

Sample	ESDD (mg/cm^2)	Leakage distance (cm)	Surface Resistance (kΩ/cm)
N2	0.15	61	60
Porcelain	0.13	61	28
N2	0.15	61	38
Porcelain	0.13	61	30
N5	0.15	109	172
Porcelain	0.15	109	20
N2 (Recovery)	0.15	61	81
N6	0.32	61	243
N5 (Recovery)	0.15	109	349
Porcelain	0.38	61	22
Porcelain	0.37	61	20
N4	0.5	61	41
Porcelain	0.3	109	81
N7	0.33	109	22
N6	0.33	61	33
Porcelain	0.55	109	7
Porcelain	0.47	109	47
N4	0.5	109	61
N4 (Recovery)	0.5	109	162
Porcelain	0.1	183	73
Porcelain	0.3	183	59
Porcelain	0.5	183	48
N1	0.1	183	98
N1 (Recovery)	0.1	183	164
N2	0.3	183	90
N2(Recovery)	0.3	183	148
N3	0.5	183	62
N3(Recovery)	0.5	183	83
N2	0.3	183	83
N2 (Recovery)	0.5	183	98
N2	0.1	183	181
N2 (Recovery)	0.1	183	213
N3	0.3	183	76
N3 (Recovery)	0.3	183	96
N1	0.5	183	76
N1(Recovery)	0.5	183	94

Sample	ESDD (mg/cm^2)	Leakage distance (cm)	Surface Resistance (kΩ/cm)
N4	0.5	109	160
Porcelain	0.5	109	95
N5	0.1	109	110
Porcelain	0.1	109	77